

Cellwise Robust Discriminant Analysis

Fabio Centofanti¹, Can Hakan Dağdır¹, Mia Hubert¹, and
Peter J. Rousseeuw¹

¹*Section of Statistics and Data Science, Department of Mathematics, KU Leuven, Belgium*

May 28, 2026

Abstract

Classical discriminant analysis (DA) is based on the mean and empirical covariance matrix of each class, both of which are sensitive to outliers in the data. In the past the focus was on casewise outliers, that is, datapoints that lie far away. But nowadays there is increasing interest in cellwise outliers, that are unexpected entries in the data matrix. Removing an entire case because it has one or a few outlying cells would lose much information. Cellwise robust methods aim to detect the outlying cells and to preserve the information in the other cells. We propose a DA method that is trained by estimating the location and covariance of each class by cellwise and casewise robust estimators, that can also handle NA's. The main novelty of our approach is in the prediction on test data, that may contain outlying cells and NA's themselves. The new robust discriminant function is derived from a novel statistical model by penalized maximum likelihood. We focus on quadratic DA, but also cover the setting of linear DA. The new cellQDA and cellLDA methods perform well in simulation. The approach is illustrated on real data, and the results are interpreted with the help of graphical displays.

Keywords: Cellwise outliers, Linear discriminant analysis, Quadratic discriminant analysis, Robust statistics, Supervised classification.

1 Introduction

Discriminant analysis (DA) is a supervised classification method for multivariate data. Classical Linear Discriminant Analysis (LDA) and Classical Quadratic Discriminant Analysis (QDA) are derived under the assumption of multivariate normal classes. In this setting, the center of a class is estimated by its arithmetic mean, and its scatter matrix is estimated by its empirical covariance matrix. However, both of these estimators are sensitive to outliers. The presence of outliers can therefore hurt the classification accuracy.

The search for robust DA methods has traditionally focused on casewise outliers, that is, cases that lie far from the majority of their class. Substantial progress has been made in this area by inserting robust estimates of the center and scatter matrix of each class, as done by He and Fung (2000), Croux and Dehon (2001), Hubert and Van Driessen (2004), Filzmoser et al. (2012), Pinheiro et al. (2025), and Becquart et al. (2026).

Casewise robust methods downweight or discard entire rows of the data matrix, which is appropriate when the outlying cases are members of a different population. But in recent times people have become aware that there is also another common type of contamination, the so-called cellwise outliers. In that setting only a few cells (entries) of a case may be suspect, while the remaining entries still contain valuable information. Even a relatively small percentage of outlying cells in the data matrix can pollute over half of the cases. When that happens, casewise robust estimators may be ineffective. Moreover, an outlying cell may be difficult to detect, as it does not have to be a marginal outlier: it suffices that its value differs markedly from what would be expected based on the relations between the variables. For instance, a child’s weight may be unremarkable by itself, but incompatible with its age and height.

Therefore there is a growing need for methods to detect outlying cells and/or provide robust estimates when they occur. In particular, cellwise robust discriminant analysis has received limited attention in the literature, in spite of the practical importance of this problem. A notable exception is Aerts and Wilms (2017), who estimated the scatter matrix of each class by the cellwise robust method of Croux and Öllerer (2016). This approach yielded a robustly trained DA model. However, it did not yet provide a robust out-of-sample prediction method. Such a mechanism would be very useful when dealing with test

data that themselves contain outlying cells.

To illustrate this issue, Figure 1 shows a toy example with three classes. Suppose that the training data was clean, so that the centers and covariance matrices of the classes are accurate. They yield the tolerance ellipses in the plot, and the quadratic boundaries of QDA shown as curved lines. The points in the figure are out-of-sample new data. Point **a** of class 2 has an outlying cell in its second variable so it ends up higher, in the decision region of class 1. Therefore the usual discriminant rule would assign it to class 1, even though it is far away from that class as well. Similarly, point **b** of class 3 would be assigned to class 2 due to its outlying cell in the first variable. Our task is to come up with an approach to assign points with outlying cells to the right class, also in higher dimensions where visual inspection would not suffice. We will revisit this example later.

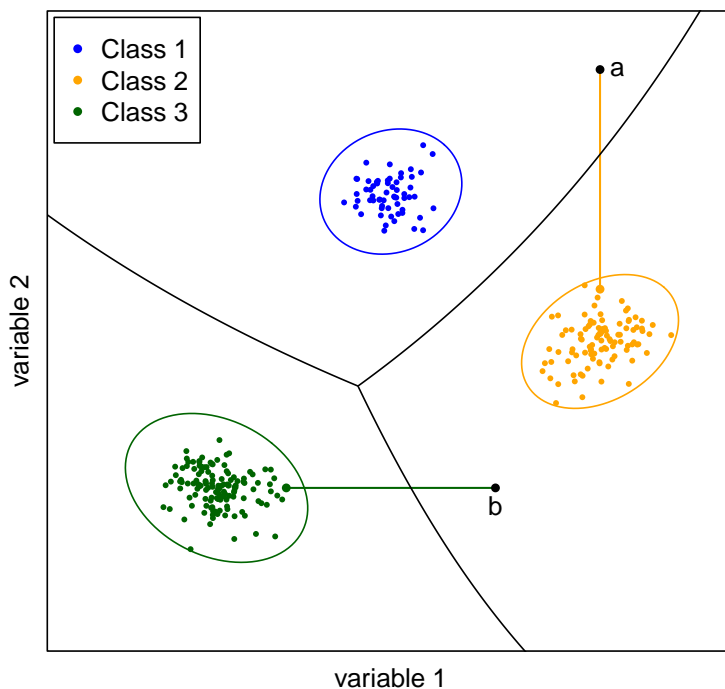


Figure 1: Illustrative example with 3 classes and their QDA boundaries. The out-of-sample points **a** and **b** each contain an outlying cell. The usual discriminant rule would misclassify them.

In this paper we propose a new cellwise robust approach to both LDA and QDA, that we will call cellLDA and cellQDA. Our methodology addresses both stages of the classification pipeline. In the training phase, we use the recent cellwise MCD estimator of Raymaekers and Rousseeuw (2024) to obtain a location and scatter matrix of each class.

The main novelty of our work is in the second stage, where our out-of-sample prediction method can handle outlying cells in the test data. For this purpose it adopts a new statistical model that extends the existing cellwise contamination model. After fitting this model on the training data, it is applied out-of-sample by flagging outlying cells in new cases, and using a new robust discriminant function. It is worth noting that all the components of this approach, from the estimation of the centers and the covariance matrices in training, to the flagging of outlying cells out-of-sample, and the derivation of the new discriminant function, are all based on the same penalized maximum likelihood. Due to this unification, the approach also handles missing values in a natural way.

To enhance interpretability, we also provide a graphical display that enables users to visually distinguish between clean cases, cases that are classified correctly despite some outlying cells, and casewise outliers.

The remainder of the paper is organized as follows. Section 2 describes the proposed methodology for in-sample and out-of-sample data. Section 3 evaluates the performance of cellLDA and cellQDA through simulation, under various contamination scenarios. Section 4 illustrates the approach on a real dataset of nutritional values. Section 5 concludes.

2 Methodology

Suppose we have training data with G classes $g = 1, \dots, G$. Each class contains d -variate points $\boldsymbol{x}_{g,i}$ for $i = 1, \dots, n_g$, and $n = \sum_{g=1}^G n_g$. The goal of discriminant analysis (DA) is to construct a classification rule based on the training data, that generalizes well to new data.

2.1 Classical discriminant analysis

The classical framework assumes that each class g contains d -variate points that were generated by a multivariate normal distribution. Formally, it assumes that the random vector \mathcal{X} follows the generative model

$$\mathcal{X} | (\mathcal{G} = g) \sim \mathcal{N}(\boldsymbol{\mu}_g, \boldsymbol{\Sigma}_g) \quad \text{with} \quad P(\mathcal{G} = g) = \pi_g$$

where $\boldsymbol{\mu}_g$ and $\boldsymbol{\Sigma}_g$ are the class-specific location vector and scatter matrix. This is called a normal mixture model. The random variable \mathcal{G} is the class membership, so $\pi_g > 0$ is the prior probability of class g , with $\sum_{g=1}^G \pi_g = 1$.

The general form of this model allows each class to have its own parameters $\boldsymbol{\mu}_g$ and $\boldsymbol{\Sigma}_g$. In this setting the discriminant function of class g in a d -variate case \boldsymbol{x} is

$$\delta_g^{\text{QDA}}(\boldsymbol{x}) = -\frac{1}{2} \log |\boldsymbol{\Sigma}_g| - \frac{1}{2}(\boldsymbol{x} - \boldsymbol{\mu}_g)^\top \boldsymbol{\Sigma}_g^{-1}(\boldsymbol{x} - \boldsymbol{\mu}_g) + \log \pi_g. \quad (1)$$

The classifier then assigns the case \boldsymbol{x} to the class g with the highest $\delta_g^{\text{QDA}}(\boldsymbol{x})$. This is called Quadratic Discriminant Analysis (QDA) because the discriminant function is quadratic in \boldsymbol{x} . It yields curved decision boundaries between classes.

In practice, estimating a separate covariance matrix $\boldsymbol{\Sigma}_g$ for each class is infeasible when some classes contain too few cases. A common approach is then to assume a shared covariance matrix $\boldsymbol{\Sigma}$ across classes, that is, $\boldsymbol{\Sigma}_g = \boldsymbol{\Sigma}$ for all g . Under this homogeneity assumption, the discriminant function simplifies to

$$\delta_g^{\text{LDA}}(\boldsymbol{x}) = \boldsymbol{x}^\top \boldsymbol{\Sigma}^{-1} \boldsymbol{\mu}_g - \frac{1}{2} \boldsymbol{\mu}_g^\top \boldsymbol{\Sigma}^{-1} \boldsymbol{\mu}_g + \log \pi_g, \quad (2)$$

as the terms $-\frac{1}{2} \log |\boldsymbol{\Sigma}_g| - \frac{1}{2} \boldsymbol{x}^\top \boldsymbol{\Sigma}^{-1} \boldsymbol{x}$ have dropped out because they do not depend on g . Now the discriminant function is linear in \boldsymbol{x} , so this method is referred to as Linear Discriminant Analysis (LDA). It yields linear decision boundaries.

The classical estimators of $(\boldsymbol{\mu}_g, \boldsymbol{\Sigma}_g)$ are the mean and the empirical covariance matrix. Both are sensitive to cellwise outliers, and so are the discriminant functions (1)–(2). We therefore need to (i) robustly estimate the class parameters in training, and (ii) construct a discriminant rule that is robust against cellwise contamination in new data.

2.2 Robustly estimating class characteristics

In the QDA setting, we will estimate the class parameters by the cellMCD method of Raymaekers and Rousseeuw (2024). Consider a class g with members $\boldsymbol{x}_{g,i}$ for $i = 1, \dots, n_g$.

On it, cellMCD optimizes an objective function to estimate $(\boldsymbol{\mu}_g, \boldsymbol{\Sigma}_g)$ as well as an $n_g \times d$ binary matrix \boldsymbol{W}_g . The i th row $\boldsymbol{w}_{g,i}$ of \boldsymbol{W}_g has $w_{g,ij} = 0$ when the cell $x_{g,ij}$ is flagged as outlying or NA, and $w_{g,ij} = 1$ indicates that it is unflagged. We denote the set of indices

of the flagged cells in case i as $m_i := m(\mathbf{w}_{g,i}) = \{j : w_{g,ij} = 0\}$ and that of the unflagged cells as $o_i := o(\mathbf{w}_{g,i}) = \{j : w_{g,ij} = 1\}$. With this notation, cellMCD minimizes

$$\sum_{i=1}^{n_g} \left(\log |\Sigma_g^{(o_i)}| + |o_i| \log(2\pi) + \text{MD}^2(\mathbf{x}_{g,i}, \mathbf{w}_{g,i}, \boldsymbol{\mu}_g, \Sigma_g) \right) + \sum_{j=1}^d q_{gj} \|\mathbf{1}_{n_g} - (\mathbf{W}_g)_{\cdot j}\|_0 \quad (3)$$

under the constraints $\lambda_{\min}(\Sigma_g) \geq a > 0$ and

$$\|(\mathbf{W}_g)_{\cdot j}\|_0 \geq h_g \text{ for all } j = 1, \dots, d.$$

Here the superscript (o_i) restricts a vector or square matrix to indices j in o_i , the number of unflagged cells of $\mathbf{x}_{g,i}$ is $|o_i|$, and

$$\text{MD}^2(\mathbf{x}_{g,i}, \mathbf{w}_{g,i}, \boldsymbol{\mu}_g, \Sigma_g) := (\mathbf{x}_{g,i}^{(o_i)} - \boldsymbol{\mu}_g^{(o_i)})^\top (\Sigma_g^{(o_i)})^{-1} (\mathbf{x}_{g,i}^{(o_i)} - \boldsymbol{\mu}_g^{(o_i)})$$

is the partial squared Mahalanobis distance. Note that the first sum is the usual observed negative log-likelihood for incomplete data. Moreover, $\mathbf{1}_{n_g}$ is a column vector of n_g ones, and $(\mathbf{W}_g)_{\cdot j}$ is the j th column of \mathbf{W}_g . Therefore $\|\mathbf{1}_{n_g} - (\mathbf{W}_g)_{\cdot j}\|_0$ is the number of flagged cells in the j th variable of class g . The $q_{gj} > 0$ are tuning parameters. The $\lambda_{\min}(\Sigma_g)$ in the first constraint is the smallest eigenvalue of Σ_g , so Σ_g is positive definite. It follows that for any square submatrix $\Sigma_g^{(o)}$ with nonempty set o and any $\mathbf{x}^{(o)} \neq \mathbf{0}$ we have $(\mathbf{x}^{(o)})^\top \Sigma_g^{(o)} \mathbf{x}^{(o)} = (\mathbf{x}^*)^\top \Sigma_g \mathbf{x}^* \geq \lambda_{\min}(\Sigma_g) \|\mathbf{x}^*\|^2 = \lambda_{\min}(\Sigma_g) \|\mathbf{x}^{(o)}\|^2$ where the d -variate vector \mathbf{x}^* has the cells of $\mathbf{x}^{(o)}$ in the positions of o and zeroes in the other positions. Therefore $\lambda_{\min}(\Sigma_g^{(o)}) \geq \lambda_{\min}(\Sigma_g)$, so all $|\Sigma_g^{(o_i)}| > 0$ and all $\text{MD}^2(\mathbf{x}_{g,i}, \mathbf{w}_{g,i}, \boldsymbol{\mu}_g, \Sigma_g)$ in (3) exist. The second constraint enforces that at least h_g cells remain unflagged in each column, where by default $h_g = \lceil 0.75n_g \rceil$. The cellMCD method is available in the R package `cellwise` (Raymaekers and Rousseeuw, 2025), and has been applied to cluster analysis by Zaccaria et al. (2025, 2026).

In the LDA setting, we estimate the shared scatter matrix Σ by pooling. We first compute the location estimate $\hat{\boldsymbol{\mu}}_g$ of each class g as the coordinatewise mean of its data imputed by the Detect Deviating Cells method (Rousseeuw and Van den Bossche, 2018). Next, we compute $\hat{\Sigma}$ by applying the cellMCD with fixed center $\mathbf{0}$ to the pooled set of all $\mathbf{x}_{g,i} - \hat{\boldsymbol{\mu}}_g$, and we use $\hat{\Sigma}$ in each class. (Note that there are other ways to regularize the $\hat{\Sigma}_g$ when some classes have too few members. For instance, we could apply cellMCD to the classes that do have enough members, and in the small classes use a weighted average of those $\hat{\Sigma}_g$ with weights n_g .)

2.3 Flagging cells in test data

Even with robust estimates of $(\boldsymbol{\mu}_g, \boldsymbol{\Sigma}_g)$, the discriminant rules in (1) and (2) cannot robustly classify new data points with cellwise contamination. That is because the discriminant rule (1) is quadratic in \boldsymbol{x} and (2) is linear in \boldsymbol{x} , so outlying cells in \boldsymbol{x} can have a large effect. Therefore we need to detect outliers in new data when classifying them. For this purpose we propose a likelihood-based *cellflagger*.

Given $(\hat{\boldsymbol{\mu}}_g, \hat{\boldsymbol{\Sigma}}_g)$ and a single point \boldsymbol{x} , cellflagger obtains a vector \boldsymbol{w}_g by minimizing the penalized objective

$$\mathcal{Q}(\boldsymbol{w}) = \log |\hat{\boldsymbol{\Sigma}}_g^{(o(\boldsymbol{w}))}| + |o(\boldsymbol{w})| \log(2\pi) + \text{MD}^2(\boldsymbol{x}, \boldsymbol{w}, \hat{\boldsymbol{\mu}}_g, \hat{\boldsymbol{\Sigma}}_g) + \sum_{j \text{ in } m} q_{gj} \quad (4)$$

that is a part of the cellMCD objective (3) but now applied to \boldsymbol{x} . Flagging a previously unflagged cell x_j decreases the objective by

$$\begin{aligned} \Delta_{gj} &= \mathcal{Q}(\boldsymbol{w} : w_j = 1) - \mathcal{Q}(\boldsymbol{w} : w_j = 0) \\ &= \log |\hat{\boldsymbol{\Sigma}}_g^{(o)}| - \log |\hat{\boldsymbol{\Sigma}}_g^{(o-j)}| + \log(2\pi) + \text{MD}^2(x_j, \hat{x}_{gj}, C_{gj}) - q_{gj} \\ &= \log C_{gj} + \log(2\pi) + \frac{(x_j - \hat{x}_{gj})^2}{C_{gj}} - q_{gj}, \end{aligned} \quad (5)$$

where $o-j$ denotes the set $o \setminus \{j\}$. Here $\hat{x}_{gj} = \hat{\boldsymbol{\mu}}_{gj} + (\hat{\boldsymbol{\Sigma}}_g)_{j,o-j} (\hat{\boldsymbol{\Sigma}}_g^{(o-j)})^{-1} (\boldsymbol{x}_{o-j} - (\hat{\boldsymbol{\mu}}_g)_{o-j})$ is the conditional expectation of cell x_j and $C_{gj} = (\hat{\boldsymbol{\Sigma}}_g)_{j,j} - (\hat{\boldsymbol{\Sigma}}_g)_{j,o-j} (\hat{\boldsymbol{\Sigma}}_g^{(o-j)})^{-1} (\hat{\boldsymbol{\Sigma}}_g)_{o-j,j}$ is the conditional variance of x_j . The squared Mahalanobis distance of the univariate x_j from the center \hat{x}_{gj} relative to the variance C_{gj} is simply $(x_j - \hat{x}_{gj})^2 / C_{gj}$. Cellflagger iteratively flags cell $j^* = \text{argmax}_j \Delta_{gj}$ if $\Delta_{gj^*} \geq 0$, updates o accordingly, and repeats until $\max_j \Delta_{gj} < 0$.

We need to set q_{gj} so that Δ_{gj} effectively filters outlying cells. If a cell is outlying, its squared standardized residual $(x_j - \hat{x}_{gj})^2 / C_{gj}$ in (5) tends to be large. As a cutoff we can use the chi-squared quantile $\chi_{1,0.99}^2$ with one degree of freedom and probability 0.99. We wish to flag a cell when its residual is too large, so we set

$$q_{gj} = \chi_{1,0.99}^2 + \log(2\pi) + \log(C_{gj}) \quad (6)$$

be default. From (5) and (6) we see that a cell x_j is flagged with respect to group g iff it lies outside a robust tolerance interval around its conditional expectation \hat{x}_{gj} with coverage 99%.

2.4 Robust discriminant function

Classifying a new case \mathbf{x} requires choosing between G classes. This creates a conundrum: for every class, the cellflagger will flag some cells of \mathbf{x} until the remainder of \mathbf{x} is not outlying for that class, hence several classes may appear to fit \mathbf{x} . To resolve this we will define a robust discriminant function based on the likelihood of \mathbf{x} in a contamination model. For any potential class, it will naturally penalize based on how many cells of \mathbf{x} need to be flagged before it looks likely to belong to that class, and on how outlying the flagged cells are from that class.

For this novel situation we need to create a suitable cellwise contamination model. The new model generates potentially contaminated data points as i.i.d. realizations of a d -variate random vector \mathcal{X} of the form

$$\begin{aligned} \mathcal{X} &= \mathcal{W} \odot \mathcal{Y} + (\mathbf{1}_d - \mathcal{W}) \odot \mathcal{Z} \quad \text{where} \\ \mathcal{Y} | (\mathcal{G} = g) &\sim \mathcal{N}(\boldsymbol{\mu}_g, \boldsymbol{\Sigma}_g) \quad \text{for } g = 1, \dots, G \\ (\mathcal{Z})_j | (\mathcal{G} = g) &\sim \text{Laplace}(\mu_{gj}, \alpha_{gj}) \quad \text{for } j = 1, \dots, d \\ (\mathcal{W})_j | (\mathcal{G} = g) &\sim \text{Bernoulli}(1 - p_{gj}) \quad \text{for } j = 1, \dots, d \\ (\mathcal{W}, \mathcal{Y}, \mathcal{Z}) &\text{ are mutually independent conditional on } \mathcal{G}. \end{aligned} \tag{7}$$

Here \odot denotes the Hadamard product that multiplies vectors entry by entry. The d -variate random vector \mathcal{Y} is the regular term, \mathcal{Z} is the contamination term with independent coordinates, and \mathcal{W} is binary with independent coordinates. The distribution $\text{Laplace}(\mu_{gj}, \alpha_{gj})$ has density $\exp(-|z_j - \mu_{gj}|/\alpha_{gj})/(2\alpha_{gj})$.

This model says that a cell at feature j is outlying for class g with probability p_{gj} . The values in outlying cells are independent for each feature-class pair, and they follow a heavier tailed distribution than the clean cells. The model (7) extends that of Alqallaf et al. (2009) to several classes, and adds a distributional model on \mathcal{Z} , that we need to perform out-of-sample predictions on contaminated data.

Under the contamination model (7), the joint likelihood of \mathcal{X} and \mathcal{W} for a given class g can be factorized as

$$f_{(\mathcal{X}, \mathcal{W}) | \mathcal{G}}((\mathbf{x}, \mathbf{w}) | g) = f_{\mathcal{W} | \mathcal{G}}(\mathbf{w} | g) f_{\mathcal{X} | (\mathcal{W}, g)}(\mathbf{x} | (\mathbf{w}, g)). \tag{8}$$

Writing $o(\mathbf{w}) = \{j : w_j = 1\}$ and $m(\mathbf{w}) = \{j : w_j = 0\}$, the contamination model implies $\mathcal{X}^{(o(\mathbf{w}))} = \mathcal{Y}^{(o(\mathbf{w}))}$ and $\mathcal{X}^{(m(\mathbf{w}))} = \mathcal{Z}^{(m(\mathbf{w}))}$, hence the second factor becomes

$$f_{\mathcal{X}|(\mathcal{W}, \mathcal{G})}(\mathbf{x}|\mathbf{w}, g) = f_{\mathcal{Y}^{(o(\mathbf{w}))}| \mathcal{G}}(\mathbf{x}^{(o(\mathbf{w}))}|g) f_{\mathcal{Z}^{(m(\mathbf{w}))}| \mathcal{G}}(\mathbf{x}^{(m(\mathbf{w}))}|g). \quad (9)$$

Combining these equations yields

$$\begin{aligned} f_{(\mathcal{X}, \mathcal{W})| \mathcal{G}}((\mathbf{x}, \mathbf{w})|g) &= f_{\mathcal{W}| \mathcal{G}}(\mathbf{w}|g) f_{\mathcal{Y}^{(o(\mathbf{w}))}| \mathcal{G}}(\mathbf{x}^{(o(\mathbf{w}))}|g) f_{\mathcal{Z}^{(m(\mathbf{w}))}| \mathcal{G}}(\mathbf{x}^{(m(\mathbf{w}))}|g) \\ &= \prod_{j=1}^d [(1 - p_{gj})^{w_j} p_{gj}^{(1-w_j)}] \phi_{(o(\mathbf{w}))}(\mathbf{x}^{(o(\mathbf{w}))} | (\boldsymbol{\mu}_g^{(o(\mathbf{w}))}, \boldsymbol{\Sigma}_g^{(o(\mathbf{w}))})) \\ &\quad \prod_{j \text{ in } m(\mathbf{w})} \frac{\exp(-|x_j - \mu_{gj}|/\alpha_{gj})}{2\alpha_{gj}}, \end{aligned} \quad (10)$$

where $\phi_{(o(\mathbf{w}))}$ is the multivariate normal density over the features in $o(\mathbf{w})$. Multiplying this density by the estimated prior probability $\hat{\pi}_g = n_g/n$ of class g , and taking the logarithm, yields the robust discriminant function

$$\begin{aligned} \delta_g(\mathbf{x}, \mathbf{w}_g) &:= \log \hat{\pi}_g + \log \phi_{(o(\mathbf{w}_g))}(\mathbf{x}^{(o(\mathbf{w}_g))} | (\boldsymbol{\mu}_g^{(o(\mathbf{w}_g))}, \boldsymbol{\Sigma}_g^{(o(\mathbf{w}_g))})) + \\ &\quad \sum_{j=1}^d \left[w_{gj} \log(1 - p_{gj}) + (1 - w_{gj}) \log p_{gj} \right] + \sum_{j=1}^d (1 - w_{gj}) \log \left(\frac{\exp(-|x_j - \mu_{gj}|/\alpha_{gj})}{2\alpha_{gj}} \right). \end{aligned} \quad (11)$$

When computing the discriminant function for a new case \mathbf{x} and a class g we first determine \mathbf{w}_g by the cellflagger for class g . Then we assign \mathbf{x} to the class with highest $\delta_g(\mathbf{x}, \mathbf{w}_g)$.

The robust discriminant rule (11) is the usual one, plus two new terms. We illustrate their roles with two examples. The first is the toy example of Figure 1. The classical rule would assign case **a** to class 1. However, suppose that we know that class 1 has only few outlying cells, that is, p_{11} and p_{12} are tiny, whereas class 2 has a higher probability p_{22} of an outlying cell in its second variable. Then the new term $\sum_{j=1}^2 [w_{gj} \log(1 - p_{gj}) + (1 - w_{gj}) \log p_{gj}]$ is very low for class $g = 1$, since $w_{11} = 0 = w_{12}$, and $\log p_{g1}$ and $\log p_{g2}$ are big negative values. For $g = 2$ we find instead $w_{21} = 1, w_{22} = 0$ and $\log p_{g2}$ is less extreme, so point **a** can be assigned to class 2. In Figure 2 we see that we would only need to move one cell of **a** to place it in class 2, whereas the blue arrows indicate that we would need to move both cells of **a** to get to class 1. Analogously, **b** can go to class 3 with only w_{31} being zero (green arrow), whereas placing it in class 2 would require both w_{21} and w_{22} to be zero.

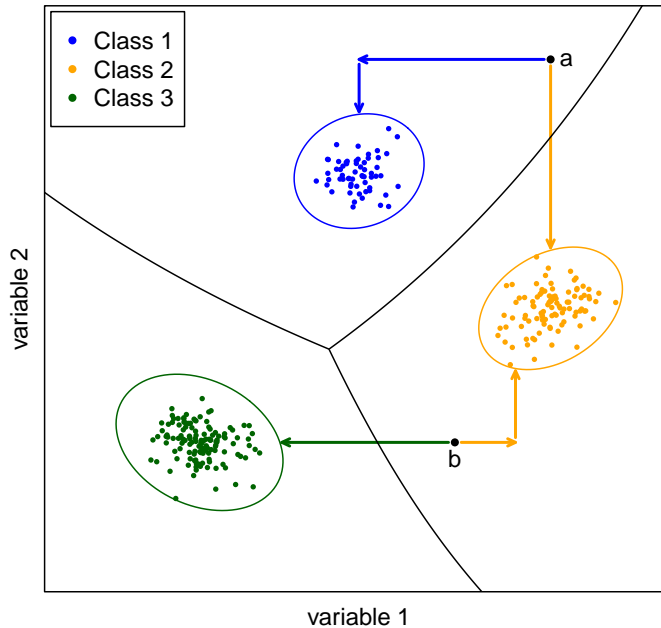


Figure 2: Assigning point **a** to class 1 yields two big negative contributions (blue arrows) in the discriminant rule (11), whereas assigning it to class 2 yields only one such term (orange arrow). Assigning point **b** to class 2 yields two such terms, against only one for class 3 (green arrow).

For the role of the second new term in (11) look at Figure 3. The variables are height and weight of males belonging to three age groups: 2–5 years old in class 1, 8–12 years in class 2, and 18–25 years in class 3. The reported height of person **c** is not particularly unusual, and neither is his weight, but the combination is quite unlikely. This may be due to an outlying cell, but is it in height or in weight? Now suppose that the Laplace parameter α_{31} is large, whereas the other five α_{gj} are tiny. That is, the spread of cellwise outliers in the height of the class of adults is large, whereas all the other spreads are small. For class 3 the final term $\sum_{j=1}^d (1 - w_{gj}) \log((\exp(-|x_j - \mu_{gj}|/\alpha_{gj})) / (2\alpha_{gj}))$ of the discriminant rule (11) has $w_{31} = 0, w_{32} = 1$, and it is rather small due to the high α_{31} . For classes 1 and 2 the term takes on a large negative value due to their tiny α_{gj} , so overall the value of the discriminant rule is highest for class 3. The method thus assigns point **c** to class 3.

An important benefit of deriving the discriminant rule (11) from the cellwise contamination model (7) is its natural handling of missing data. If a case \mathbf{x} contains missing entries (NA's), we fix $w_j = 0$ in these cells, prior to the application of the cellflagger. We then permanently exclude those j from the index set $o(\mathbf{w})$ of clean cells, and from both sums over j in the discriminant function (11).

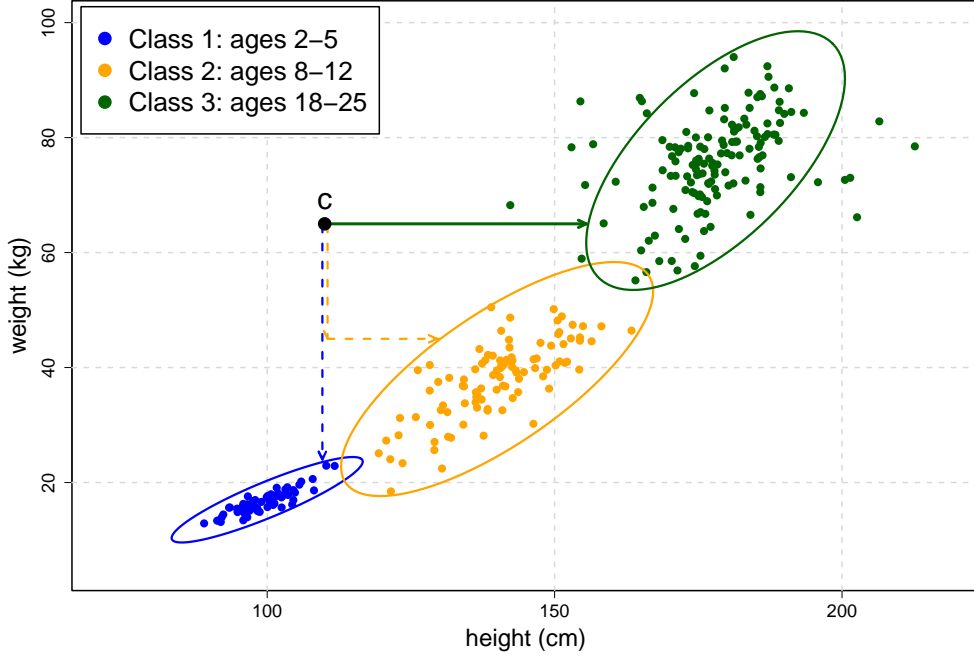


Figure 3: Illustration of how the new discriminant function (11) assigns the out-of-sample point \mathbf{c} to class $g = 3$, that has a higher spread α_{gj} of cellwise outliers in the variable Height ($j = 1$).

We now look at the situation where the new case \mathbf{x} does not belong to any of the classes, that is, it is a casewise outlier for all classes. The above method will predict some class g , with the class-specific cellflagger output \mathbf{w}_g . We will flag \mathbf{x} as a casewise outlier if the number of flagged cells $|m(\mathbf{w}_g)|$ is larger than or equal to $d/2$, or when the Mahalanobis distance $\text{MD}^2(\mathbf{x}, \mathbf{w}_g, \hat{\boldsymbol{\mu}}_g, \hat{\boldsymbol{\Sigma}}_g)$ of the remaining cells exceeds the 0.99 quantile of the χ^2 distribution with $\sum_{j=1}^d w_j$ degrees of freedom. Such overall casewise outliers are then assigned to a new class with the number 0.

2.5 Parameter estimation

Our modeling choices for \mathcal{W} and \mathcal{Z} are motivated by simplicity and transparency. Contamination at a cell is an on/off event, making Bernoulli indicators a natural choice. Also, the resulting log-likelihood expression remains separable, and yields an explicit penalty on the number of flagged cells, that is analogous to the columnwise penalty terms in the objective (3) of cellMCD and the objective (4) of the cellflagger. The Laplace model has heavier tails than the normal model, and for flagged cells it subtracts $\sum_{j=1}^d (1 - w_{gj}) [|(x_j - \mu_{gj})/\alpha_{gj}| - \log(2\alpha_{gj})]$ from the log-likelihood (11). The sum of the $|(x_j - \mu_{gj})/\alpha_{gj}| |1 - w_{gj}|$

is a weighted L_1 norm of $\mathbf{1} - \mathbf{w}$, and the sum of the $\log(2\alpha_{gj})|1 - w_{gj}|$ is a weighted L_0 pseudonorm of $\mathbf{1} - \mathbf{w}$. Both are loosely connected to the sparsity of $\mathbf{1} - \mathbf{w}$ that we saw in cellMCD and the cellflagger, where the number of flagged cells was penalized.

We estimate the contamination parameters (p_{gj}, α_{gj}) from flagged cells in the training data. That is, after computing the cellMCD estimates $(\hat{\boldsymbol{\mu}}_g, \hat{\boldsymbol{\Sigma}}_g)$ of the class parameters, we apply the cellflagger to each training case $\mathbf{x}_{g,i}$ with its given class g to obtain flags $\mathbf{w}_{g,i}$. This step is necessary because the flagging patterns from cellMCD, obtained by joint optimization over $\boldsymbol{\mu}_g, \boldsymbol{\Sigma}_g$ and \mathbf{W}_g , may differ slightly from those of the cellflagger that takes $\hat{\boldsymbol{\mu}}_g$ and $\hat{\boldsymbol{\Sigma}}_g$ as given. Moreover, this step ensures the same flagging in-sample and out-of-sample. In other words, if we encounter an in-sample $\mathbf{x}_{g,i}$ in the test dataset, it will get the same $\mathbf{w} = \mathbf{w}_{g,i}$ that it had in the training data. This makes the approach internally consistent.

We first estimate the Bernoulli parameters p_{gj} . For class g and feature j , we denote the number of flagged cells by $m_{gj} = \sum_{i=1}^{n_g} (1 - w_{g,ij})$. We estimate the contamination probability from the empirical frequency of the flagged cells:

$$\hat{p}_{gj} = \max\left(0.01, \frac{m_{gj}}{n_g}\right), \quad (12)$$

where the floor 0.01 matches the tolerance level of the cellflagger. Even when no outlying cells are generated ($p_{gj} = 0$), the cellflagger will still flag approximately 1% of cells due to its use of the quantile $\chi_{1,0.99}^2$ by default. Therefore, we set the minimal value of \hat{p}_{gj} to 0.01 in order to account for the baseline flagging rate. This was found to work well in simulation.

Next, we estimate the Laplace parameter α_{gj} . Denote the sum of absolute deviations over flagged cells as

$$S_{gj} = \sum_{i=1}^{n_g} (1 - w_{g,ij}) |x_{g,ij} - \hat{\mu}_{gj}|.$$

The maximum likelihood estimator $\hat{\alpha}_{gj}^{\text{MLE}} = \frac{S_{gj}}{m_{gj}}$ provides reliable estimates when sufficiently many cells are flagged. When no cells are flagged, we set a default scale estimate by matching the 0.995 quantiles of the Laplace and the normal distributions. This yields the default scale estimate

$$\hat{\alpha}_{gj}^{(0)} := \frac{z_{0.995}}{\log(100)} \sqrt{\frac{1}{(\hat{\boldsymbol{\Sigma}}_g^{-1})_{jj}}} \approx 0.56 \sqrt{\frac{1}{(\hat{\boldsymbol{\Sigma}}_g^{-1})_{jj}}}.$$

To stabilize the estimate of α_{gj} when m_{gj} is nonzero but small, our final estimate is a weighted average of the default estimate and the MLE:

$$\widehat{\alpha}_{gj} = \frac{\tau\alpha_{gj}^{(0)} + m_{gj}\widehat{\alpha}_{gj}^{\text{MLE}}}{\tau + m_{gj}} = \frac{\tau}{\tau + m_{gj}}\widehat{\alpha}_{gj}^{(0)} + \frac{m_{gj}}{\tau + m_{gj}}\widehat{\alpha}_{gj}^{\text{MLE}}. \quad (13)$$

This equals $\widehat{\alpha}_{gj}^{(0)}$ when $m_{gj} = 0$ and tends to $\widehat{\alpha}_{gj}^{\text{MLE}}$ for increasing m_{gj} . We set $\tau = \min(1, \frac{n_g}{100})$ to match the false positive rate of the cellflagger, that flags approximately 1% of clean cells. Capping τ at 1 serves the following purpose. We know that when 10 or more cells are flagged the MLE is stable, and for $m_{gj} \geq 10$ the weight of the default scale $\widehat{\alpha}_{gj}^{(0)}$ indeed gets small enough due to $\tau/(\tau + m_{gj}) \leq 1/(1 + m_{gj}) \leq 1/11 < 0.1$.

In the quadratic discriminant analysis setting we will use the name cellQDA for the entire procedure that includes estimation of all parameters on the training data, as well as the robust discriminant function for out-of-sample data. Its linear counterpart will be denoted cellLDA.

3 Simulations

We will evaluate the performance of discriminant analysis methods on simulated data with cellwise and/or casewise contamination. Clean data are generated from a normal mixture of $G = 3$ groups. The training and test cases in group g are sampled from $\mathcal{N}(\boldsymbol{\mu}_g, \boldsymbol{\Sigma}_g)$. For each class, we generate 200 training cases and 200 test cases. The simulations are carried out in dimensions $d = 5$ and $d = 20$.

3.1 Quadratic Discriminant Analysis

For the true $\boldsymbol{\Sigma}_g$ we use correlation matrices with decaying off-diagonal entries, such as the A09 correlation matrix that has the entries $(\boldsymbol{\Sigma}_g)_{ij} = (-0.9)^{|i-j|}$. By replacing 0.9 by other multiples of 0.1 we obtain analogous matrices like A08 and A04. We consider two scenarios, with high and low correlation. In the high-correlation scenario we set $(\boldsymbol{\Sigma}_1, \boldsymbol{\Sigma}_2, \boldsymbol{\Sigma}_3) = (\text{A09}, \text{A08}, \text{A07})$, whereas in the low-correlation scenario we use $(\boldsymbol{\Sigma}_1, \boldsymbol{\Sigma}_2, \boldsymbol{\Sigma}_3) = (\text{A06}, \text{A04}, \text{A02})$. We choose the true class centers as follows: $\boldsymbol{\mu}_1 = \mathbf{0}$, $\boldsymbol{\mu}_2 = \mathbf{1}_d$, and $\boldsymbol{\mu}_3 = \mathbf{v}$, where $\mathbf{1}_d$ is the $d \times 1$ column vector of ones and $\mathbf{v} = (2, -2, 2, -2, \dots)^\top$ is a vector with alternating signs.

We consider three contamination types. In the cellwise outlier scenario we replace 10% of random cells x_{ij} by $\mu_{gj} + \gamma\sqrt{(\Sigma_g)_{jj}}$, where γ varies from 0 to 10. When $\gamma = 0$, we do not contaminate the data. In the casewise outlier scenario, 10% of the cases in class g are generated from $\mathcal{N}(\boldsymbol{\mu}_g + \frac{\gamma}{2}(\boldsymbol{\mu}_{g'} - \boldsymbol{\mu}_g), \Sigma_g)$ where g' denotes the next class in the cyclic ordering $1 \rightarrow 2 \rightarrow 3 \rightarrow 1$. In the mixed contamination scenario, we contaminate 5% of the cells and 5% of the cases. The contaminated data are generated by the function `generateData()` in the R package `cellWise`. Each combination of scenarios is replicated 20 times.

As a baseline we include classical QDA, denoted as CQDA, which uses the mean and empirical covariance matrix of each class in its discriminant rule. To the best of our knowledge, Aerts and Wilms (2017) is the only prior work on cellwise robust QDA. They consider several approaches, and for quadratic discriminant analysis they find that the best performing one estimates the Σ_g by the cellwise robust graphical lasso. We will refer to their QDA method as GLQDA, where GL stands for Graphical Lasso. We also include the casewise robust method of Hubert and Van Driessen (2004), denoted RQDA, that estimates the $\boldsymbol{\mu}_g$ and Σ_g by the casewise MCD using the algorithm of Rousseeuw and Van Driessen (1999). RQDA is able to flag casewise outliers in the test data, and excludes them from the classification by putting them in the separate class 0.

3.1.1 Performance with clean test data

We evaluate all four methods under the three scenarios described above, where the training data contains cellwise outliers only, or casewise outliers only, or the combination of both. We then consider three different settings for the test data: without any outliers (clean), with cellwise outliers, and with casewise outliers.

We start by comparing the four methods for clean *test* data. The comparison is a bit tricky, since CQDA and GLQDA assign the test cases to a class in $\{1, 2, 3\}$, whereas RQDA and cellQDA will by default assign them to a class in $\{0, 1, 2, 3\}$ where 0 is the extra class for flagged outlying cases. Since the accuracy measure should be the same for all methods in the comparison, for now we turn off the casewise outlier detection mechanisms of RQDA and cellQDA. This forces them to assign all test cases to the same three classes $\{1, 2, 3\}$.

Figure 4 shows the resulting accuracies as a function of γ in dimension $d = 20$, with

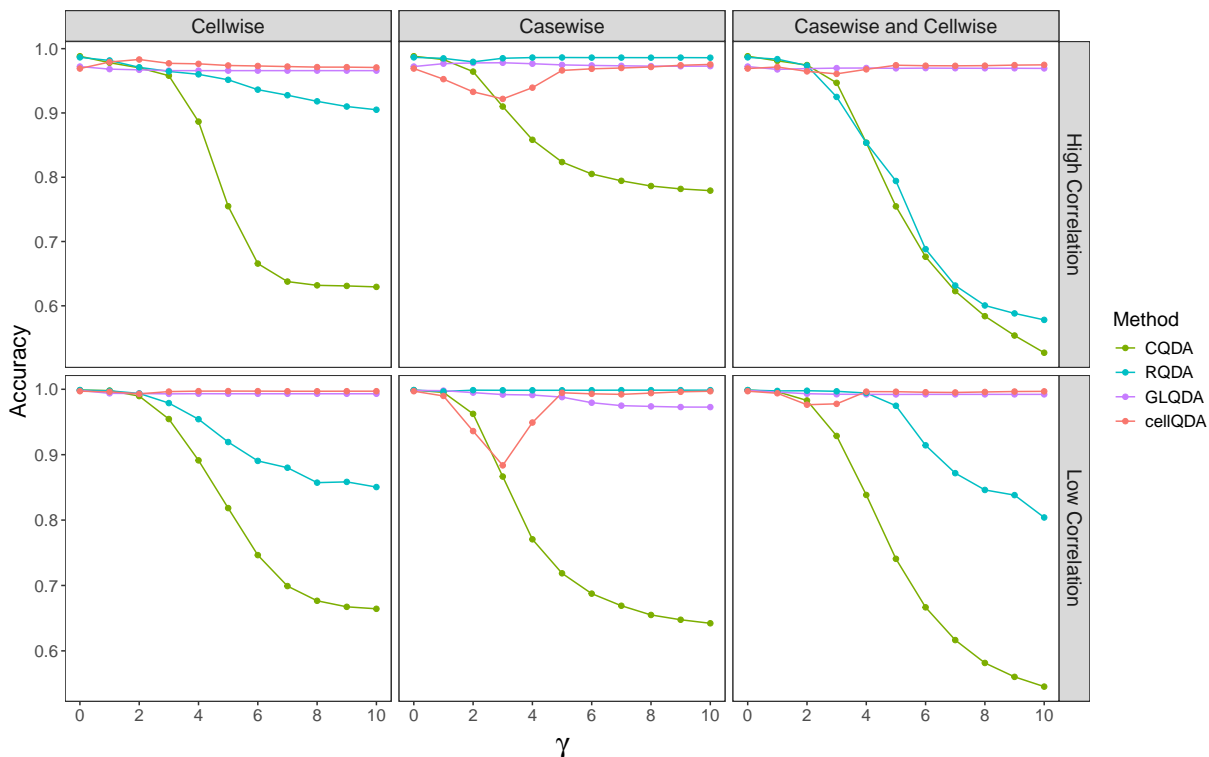


Figure 4: Accuracy of four QDA methods on 3 classes in 20 dimensions, with $n = 200$. In the top row the classes have high within correlations, and the bottom row has low within correlations. The first column uses training data with 10% of cellwise outliers only, the second with 10% of casewise outliers only, and the third with 5% of cellwise and 5% of casewise outliers. The parameter γ on the horizontal axis says how far away the outliers are. The accuracy is measured on test data that contains no contamination.

the high-correlation scenario in the top row and the low-correlation scenario in the bottom row. For clean *training* data (labeled as $\gamma = 0$), all methods attain an accuracy close to 100%. But for $\gamma > 1$ some accuracies degrade. The performance depends a lot on the type of contamination. In the first and third columns we see that whenever cellwise outliers are present in the training data, cellQDA and GLQDA are the only methods that can withstand increasing γ values. In the middle column only casewise outliers are present in the training data, and then the casewise robust method RQDA did very well, followed closely by cellQDA and GLQDA, but not CQDA.

3.1.2 Performance with cellwise outliers in the test set

With its clean test data, Figure 4 basically reflects the robustness and efficiency of the estimators of μ_g and Σ_g during training.

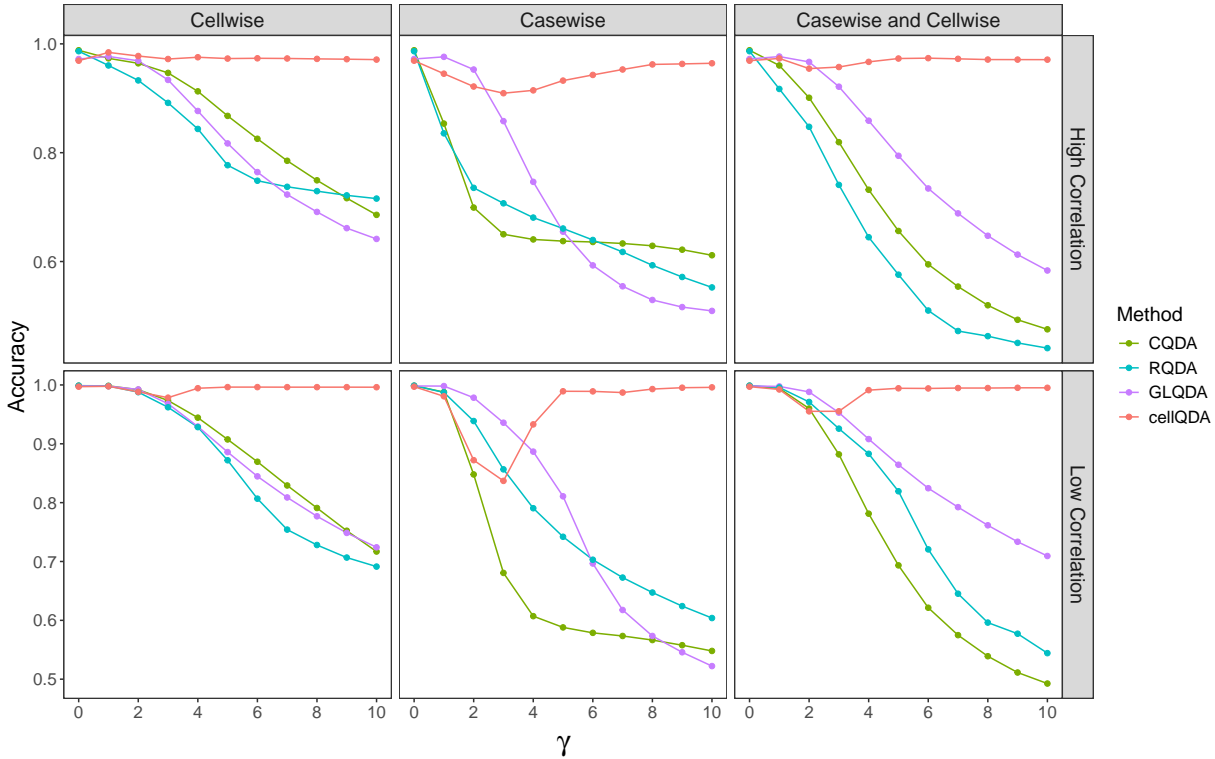


Figure 5: Comparison of the four QDA methods on the same training data as in Figure 4 and displayed in the same way. The difference is in the test data, that now contains 10% of cellwise outliers with the same γ used in training.

However, it often happens that the test data are contaminated as well, so we need to study the performance in such situations also. Figure 5 compares the methods when the test data has 10% of cellwise outliers only, with the same γ values used in the training data. Note that the training data as well as the estimates of μ_g and Σ_g stay exactly the same as before. We see that when cellwise contamination is introduced in the test set, the performance of all methods except cellQDA deteriorates substantially. When γ increases, only cellQDA remains standing. From Figure 4 we know that RQDA and GLQDA did obtain accurate estimates of the class parameters μ_g and Σ_g . Their decline here clearly demonstrates the importance of a discriminant rule that accounts for contaminated cells, as only cellQDA has that property.

3.1.3 Performance with casewise outliers in the test set

It is also possible that the test data contains casewise outliers. We now generate test data with 10% of casewise outliers with the same γ as in training, and without cellwise outliers.

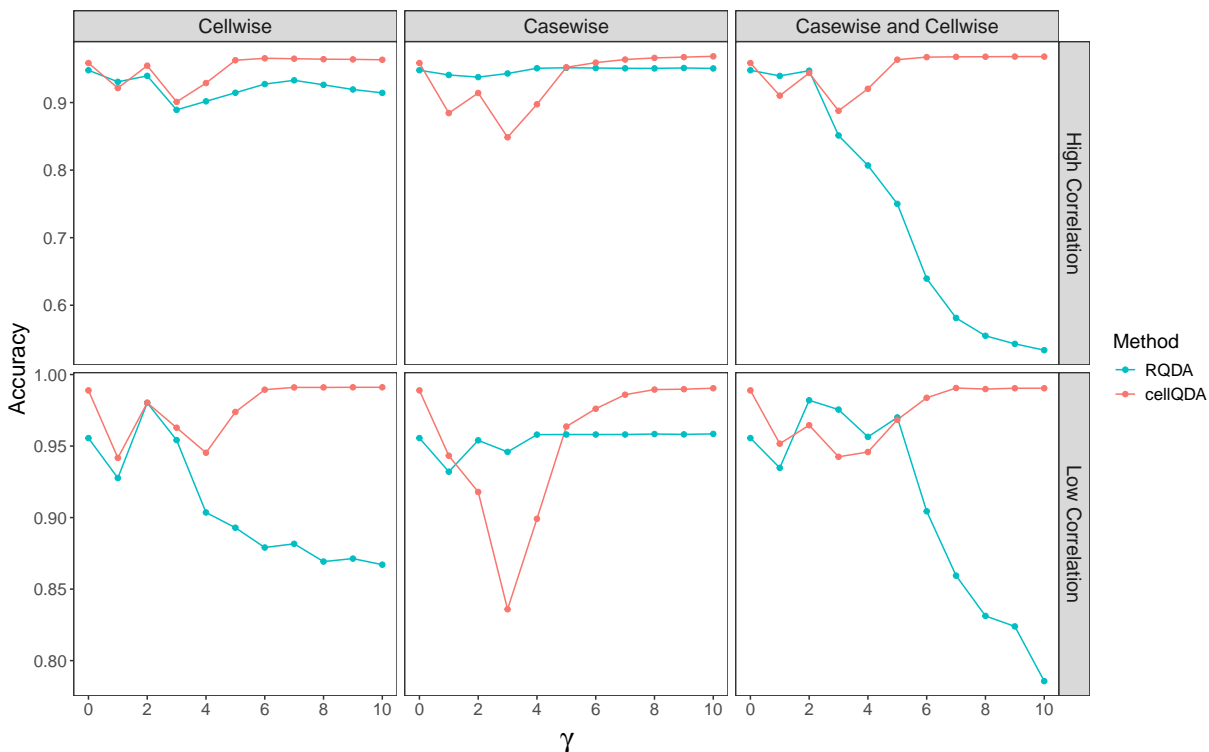


Figure 6: Comparison of RQDA and cellQDA on the same training data as in Figure 4 and displayed in the same way. Now the test data contains a class 0 with 10% of generated casewise outliers. The reported accuracy is of the assignments to the four classes 0, 1, 2, and 3.

For the computation of the accuracy, we define the true class 0 as the set of generated casewise outliers. We switch the casewise detection rules of RQDA and cellQDA back on, so they can assign flagged cases to class 0. We compute the accuracy as the number of correct assignments to the classes in $\{0, 1, 2, 3\}$, divided by the size of the test set. Since CQDA and GLQDA don't assign cases to a class 0, they are absent in this comparison.

In the middle column we see that when both the training data and the test data only have casewise outliers, cellQDA does about as well as RQDA that was designed for casewise outliers. But when the training data also contained cellwise outliers, cellQDA outperformed RQDA.

3.2 Linear Discriminant Analysis

Linear discriminant analysis assumes that all classes were generated with the same scatter matrix Σ . In our simulation we use Σ of type A09 in the high correlation scenario, and of type A06 in the low correlation setting. The class centers μ_1 , μ_2 , and μ_3 are the same as in QDA.

Our comparison includes classical LDA, denoted as CLDA. It first computes the mean $\bar{\mu}_g$ of each class g , and then estimates the shared covariance matrix Σ by the empirical covariance of the pooled centered data $\{\mathbf{x}_i - \bar{\mu}_{g_i}; i = 1, \dots, n\}$. The LDA alternative of GLQDA first computes robust estimates $\hat{\mu}_g$ and then estimates Σ by applying the cellwise robust graphical lasso to the $\mathbf{x}_i - \hat{\mu}_{g_i}$. We will refer to this method as GLLDA. We also include a casewise robust linear discriminant analysis method of Hubert and Van Driessen (2004), denoted as RLDA. They describe three different approaches. We use the version that pools classes in the same way as CLDA, cellLDA, and GLLDA. First the estimates $\hat{\mu}_g$ of the centers are obtained by the casewise MCD, and then the shared Σ is estimated by applying the casewise MCD to the $\mathbf{x}_i - \hat{\mu}_{g_i}$. Afterward a reweighting step is carried out, based on robust Mahalanobis distances, that flags casewise outliers in the training data. Next, the flagged cases are removed from the final estimates of the class centers, the shared covariance matrix, and the prior probabilities of the classes. The resulting estimates are then plugged into the linear discriminant rule. As in RQDA, cases with sufficiently large robust Mahalanobis distance are assigned to class 0.

Figure 7 shows the accuracy when the test data is contaminated with 10% of cellwise outliers, in the same way as in Figure 5. Only cellLDA holds its own when γ grows. CPCA already suffers during training, because the outliers affect the $\bar{\mu}_g$ and the empirical covariance matrix. The other methods give more robust estimates of μ and Σ , but during the out-of-sample prediction only the cellLDA discriminant rule avoids the effect of the outlying cells in the test data.

All the simulations reported here are for $d = 20$ dimensions. The results for $d = 5$ are qualitatively similar and can be found in Section A of the Supplementary Material.

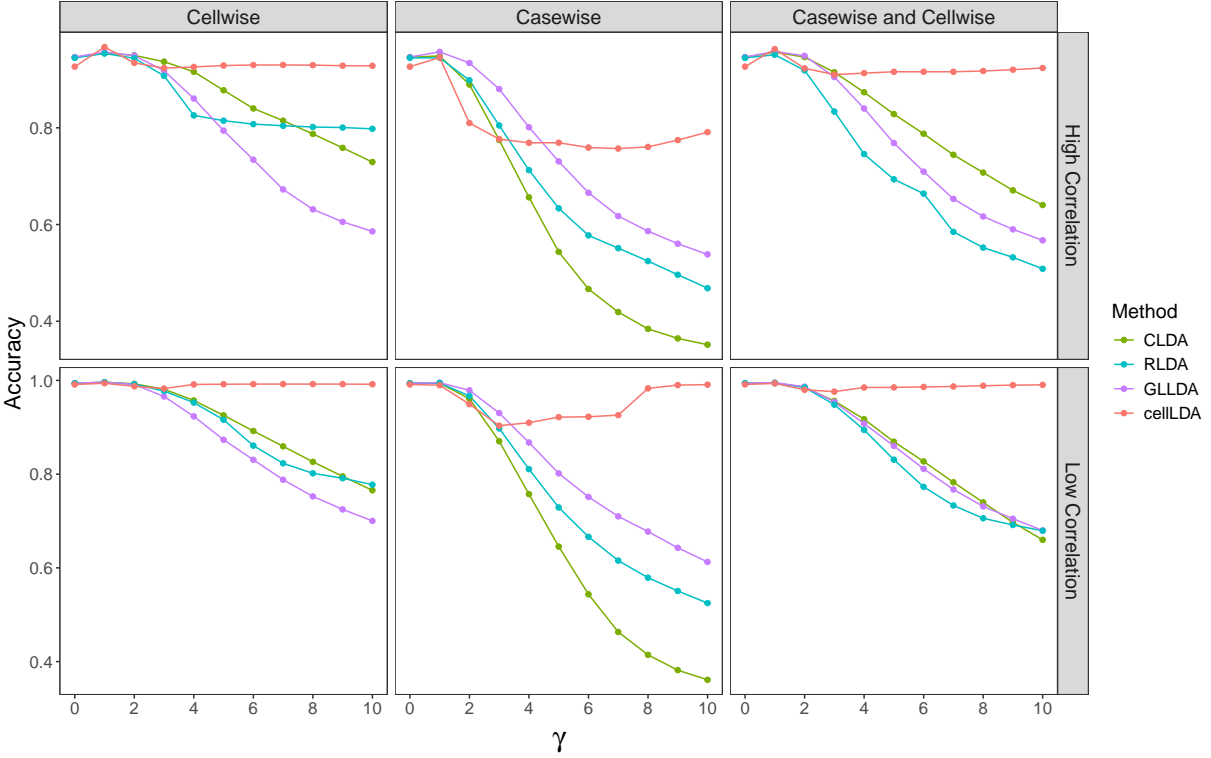


Figure 7: Comparison of four LDA methods on three classes in 20 dimensions with $n = 200$, similar to Figure 5. Now the three classes were generated with the same covariance matrix Σ , that has high correlations in the top row and low correlations in the bottom row.

4 A real data example

We will analyze a subset of the `nutrients_branded` dataset that is publicly available in the R-package `robCompositions` (Templ et al., 2020). It contains data on 804 different sweets sold in Switzerland. They are divided into four classes: “Cookies and Biscuits”, “Milk-based ice cream”, “Cakes and tarts”, and “Creams and puddings”. It has 9 variables, describing nutritional contents: energy (kcal), proteins, water, carbohydrates, sugars, dietary fibers, total fat, saturated fatty acids, and salt. The dataset was analyzed earlier by Raymaekers et al. (2022) using support vector machines. That paper found some misclassified cases and casewise outliers, and afterward interpreted them as being due to some atypical contents. Here we will instead flag cellwise outliers that directly indicate unusual contents, such as unexpectedly high salt.

We computed the out-of-sample classification accuracy of CQDA, RQDA, GLQDA, and cellQDA by 5-fold cross-validation, replicated 10 times on different random folds. The

average accuracy of cellQDA was 0.832, and exceeds those of CQDA (0.569), RQDA (0.805), and GLQDA (0.767). Figure 8 shows boxplots of the accuracies on the 10 times 5 test sets. Classical CQDA has the highest variability here.

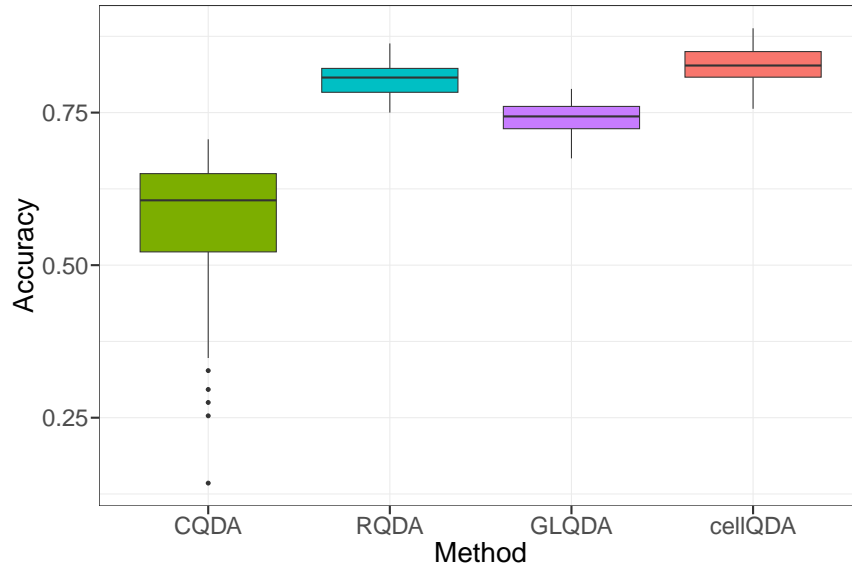


Figure 8: Boxplot of cross-validated accuracies.

We can visualize the cellQDA classification by classmaps, as introduced in Raymaekers et al. (2022). Each of the 4 classes has its own classmap. Let us focus on the classmap of the products labeled as ice cream, in the top right panel of Figure 9. For each ice cream product, the horizontal axis shows its robust Mahalanobis distance to the center of the ice cream class. These distances are labeled as their cumulative distribution values for the $\sqrt{\chi_d^2}$ distribution with $d = 9$ degrees of freedom. There is a vertical cutoff line at its 99% quantile. Moreover, the horizontal axis is not equispaced. Instead, the quantiles are spaced like those of the standard univariate normal restricted to the interval $[0, 4]$.

On the vertical axis of the classmap we see another quantity ranging from 0 to 1. This is the Probability of the Alternative Class (PAC). It is defined as follows. The posterior probability of a case i belonging to class g follows from (11):

$$\hat{p}(i, g) = \hat{\pi}_g \phi_{(o(\mathbf{w}_i))} \left(\mathbf{x}_i^{(o(\mathbf{w}_i))} \mid (\hat{\boldsymbol{\mu}}_g^{(o(\mathbf{w}_i))}, \hat{\boldsymbol{\Sigma}}_g^{(o(\mathbf{w}_i))}) \right) \prod_{j=1}^d \left[(1 - \hat{p}_{gj})^{w_{ij}} \hat{p}_{gj}^{(1-w_{ij})} \right] \prod_{j=1}^d \left(\frac{\exp(-|x_{ij} - \hat{\mu}_{gj}| / \hat{\alpha}_{gj})}{2\hat{\alpha}_{gj}} \right)^{(1-w_{ij})}.$$

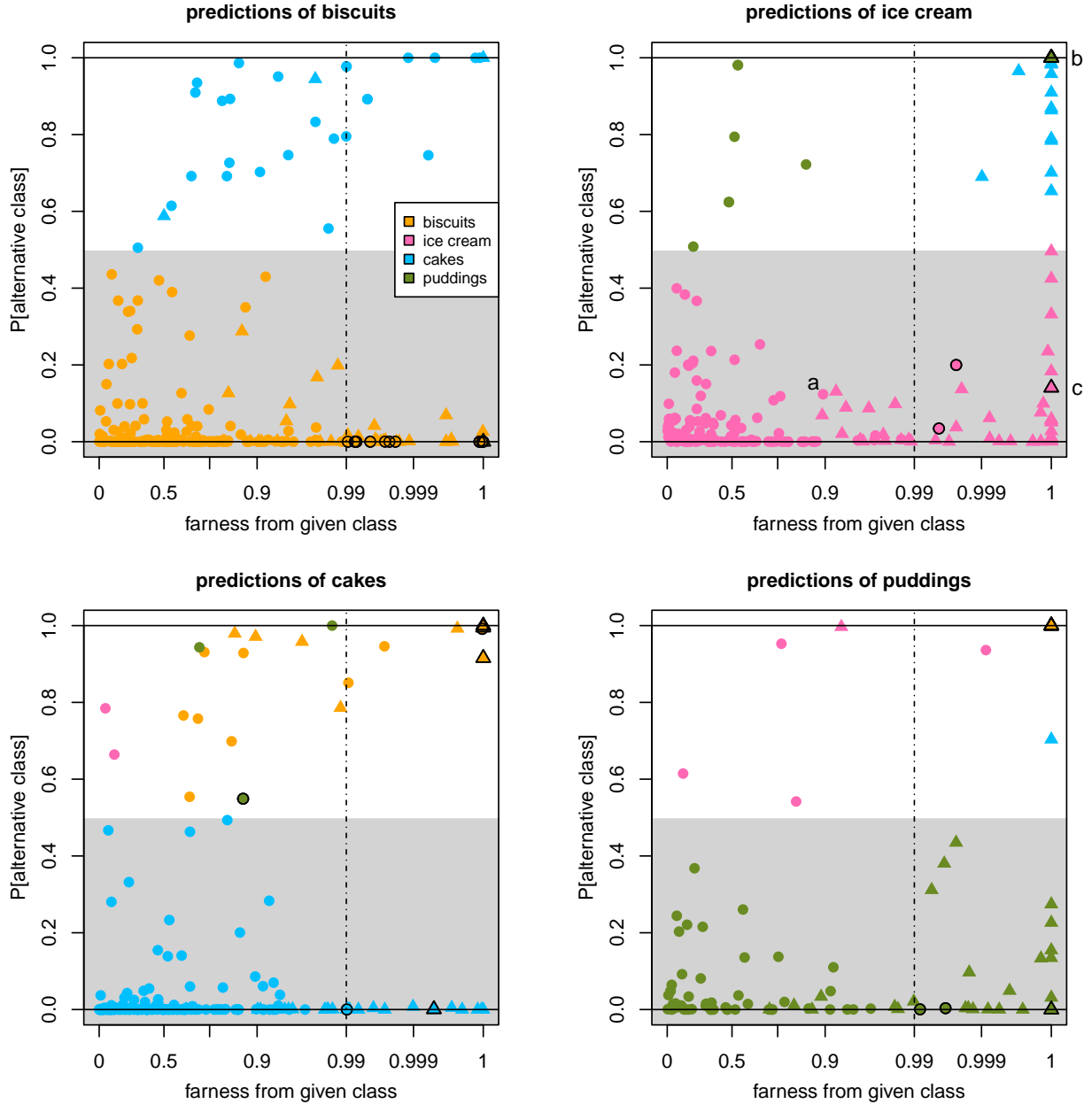


Figure 9: Class maps of the cellQDA classification of the sweets data, one map per given class. The points are colored according to their predicted class. Points with a black boundary were put in the class 0 of the flagged cases. Triangles indicate cases with at least one flagged cell.

The given label of case i is g_i , but that does not always mean that the posterior probability $\hat{p}(i, g)$ is the highest at $g = g_i$. We define the highest $\hat{p}(i, g)$ attained at a class *different from* g_i as

$$\tilde{p}(i) := \max\{\hat{p}(i, g) ; g \neq g_i\}.$$

The class attaining this maximum can be seen as the best alternative to class g_i . When

$\hat{p}(i, g_i) > \tilde{p}(i)$ we know that g_i attains the highest posterior probability in case i , so the classifier will indeed assign i to class g_i . However, when $\hat{p}(i, g_i) < \tilde{p}(i)$ the MAP rule won't assign object i to class g_i but to the best alternative class, so case i is misclassified.

We now compute the PAC as the conditional posterior probability of the best alternative class, given that we can only choose between that class and g_i . This yields

$$\text{PAC}(i) := \frac{\tilde{p}(i)}{\hat{p}(i, g_i) + \tilde{p}(i)}, \quad (14)$$

and that is plotted on the vertical axis. Note that when $\text{PAC}(i) < 0.5$ the classifier does predict the given class g_i , whereas $\text{PAC}(i) > 0.5$ means that it prefers the best alternative class instead. This natural boundary at 0.5 is why the lower half of the classmap has a light grey background: that is the region where the classifier agrees with the given label. The upper half contains the misclassified cases. All cases are colored by their predicted class. So in the lower half we only see pink points, the color of the ice cream class in the legend box. Here the misclassified points are green (puddings) or blue (cakes). The points with a black boundary are those that were put in class 0 after being assigned.

The original classmap only reflected casewise information. Here we add some cellwise information to it. Points without flagged cells are still plotted as round shapes, but now points with at least one flagged cell get a triangular shape. We see that the triangles are often on the right hand side of the classmap, as far cellwise outliers can cause large Mahalanobis distances. Point (a) is round, and lies in the regular area with a small PAC and a distance below the cutoff. Point (b) is misclassified as a pudding (green) with high conviction, as its PAC is close to 1. It is a casewise outlier with high distance, and it is a triangle so it has at least one outlying cell. Point (c) is also a casewise outlier with at least one outlying cell, but classified correctly as an ice cream.

In the bottom left panel of Figure 9 we see that many cakes are misclassified as orange points, so biscuits. Figure 10 shows the scatterplot of `carbohydrates` versus `water` content. We see that most of the cakes that are misclassified as biscuits have very low water content, that is more common for biscuits than for cakes. Most of these points correspond to cake mixes or fairly dry cakes based on nuts.

If we want to visualize more cellwise information we naturally turn to a cellmap like Figure 11. A cellmap contains a little square for each cell. The square is colored yellow

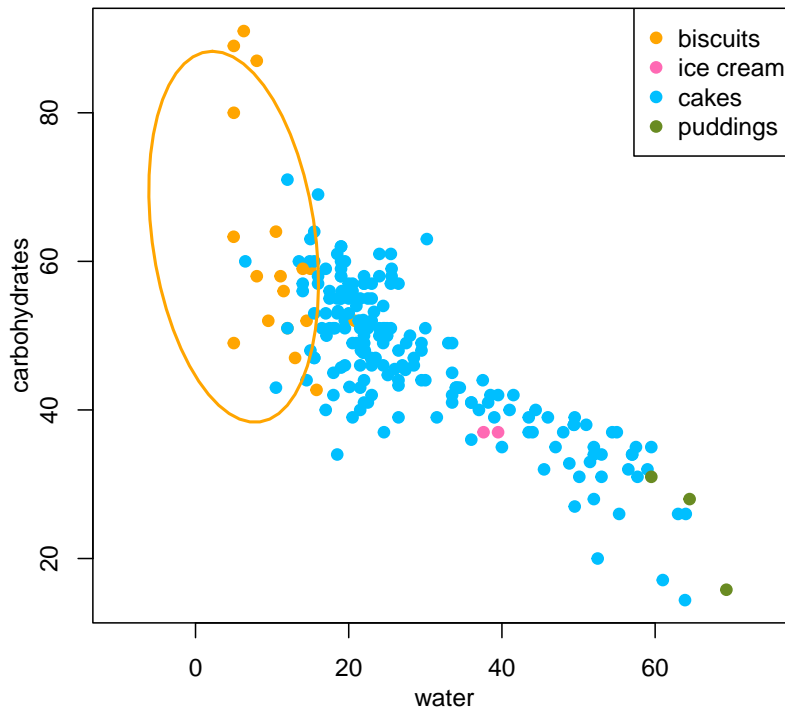


Figure 10: Scatter plot of classification results of the cakes class. Datapoints are colored by their predicted class. The tolerance ellipse of the biscuits class is shown in orange.

for unflagged cells. It is red when the cell value is unexpectedly high, and blue when it is unexpectedly low. Here, high and low are relative to the predicted value of the cell that was obtained by cellMCD in the given class. The cellmap in Figure 11 contains some selected products from the ice cream class, including the points marked (a), (b) and (c) in the classmap in Figure 9. Case (a) is regular, and none of its cells are flagged as they are all yellow. The next five products in the list are from the Weight Watchers brand. As the name suggests, this brand positions itself in the market as a healthy option. Both RQDA and cellQDA assign the Weight Watchers products to class 0. In Figure 11 we see that cellQDA flags many cells of these products due to unexpectedly low energy, high protein, low sugars, high dietary fibres, and low fat. The remaining products in the cellmap are those that were misclassified by RQDA but classified correctly by cellQDA. Looking at the cellmap, we attribute this mainly to the unexpectedly high and low salt levels.

Finally, we investigate how well cellQDA handles missing data by setting some random cells to missing in the test data. Figure 12 shows the resulting cross-validated accuracy of cellQDA for up to 60% of missing cells. For up to about 25% of NA's the accuracy

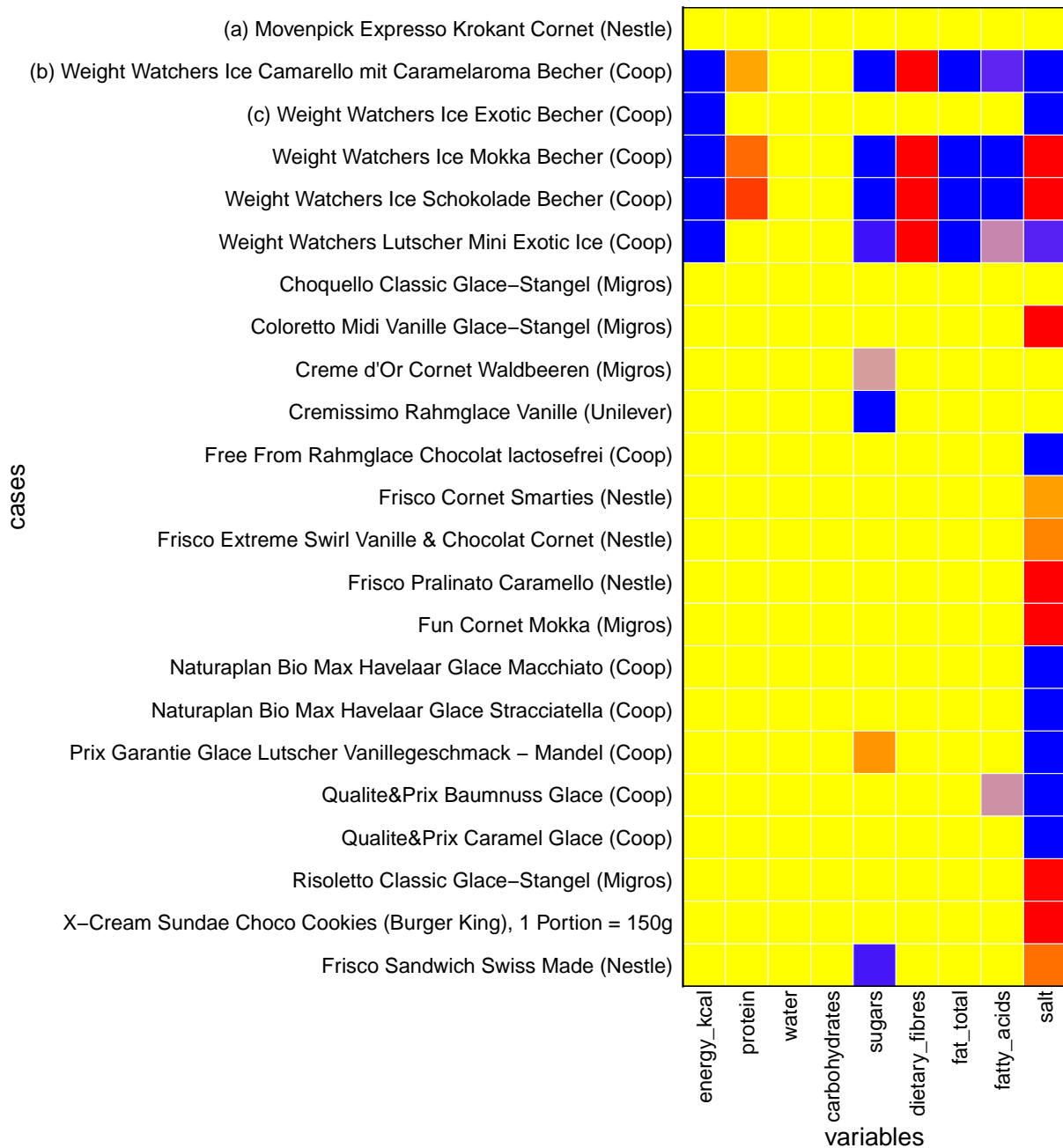


Figure 11: Cellmap of selected ice cream products. Unflagged cells are yellow. Red cells have values that are substantially higher than expected, and blue cells lower than expected. The color intensity is proportional to the magnitude of the standardized residual.

decreases only slightly, and afterward it goes down faster. But even at 60% of NA's, the 76% accuracy of cellQDA still outperforms the 57% accuracy of CQDA applied to complete test data.

Section B of the Supplementary Material provides some more results on the sweets data,

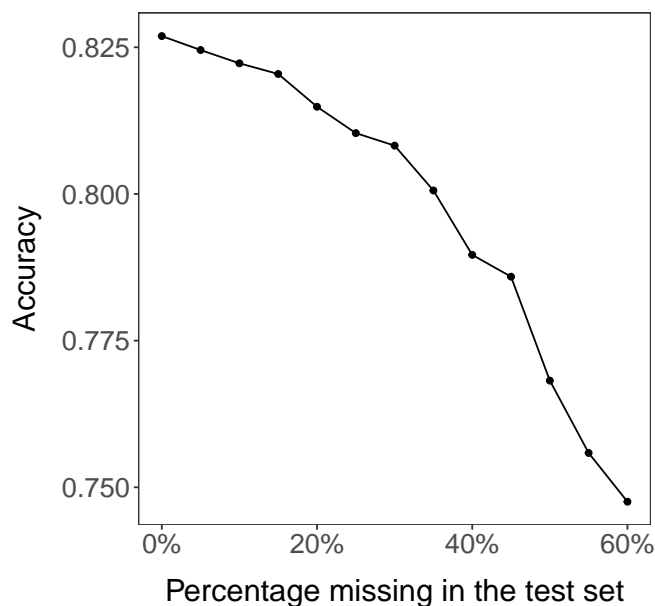


Figure 12: Cross-validated accuracy of cellQDA on the sweets data, when an increasing percentage of random cells are set to missing in the test data.

and Section C looks into two other datasets.

5 Conclusions

We have introduced the cellwise robust discriminant analysis method cellQDA and its linear counterpart cellLDA. The main novelty of our approach lies in the out-of-sample prediction stage, which is able to classify cases in the test set that contain cellwise outliers themselves. In order to achieve this we have proposed an extension of the cellwise contamination model, as well as a likelihood-based cellflagger for detecting outlying cells. The approach is coherent in that the methods to estimate the class parameters, to detect outlying cells, and to assign test cases to classes, all use the same underlying principle based on a penalized likelihood function. This also enables it to handle missing values in the data.

Extensive simulations indicate that cellQDA and cellLDA consistently outperform their classical counterparts as well as existing robust methods when cellwise outliers are present, without sacrificing performance when the data are clean or contain casewise outliers only. The methodology is illustrated on a real life dataset about the composition of food products,

and the results are interpreted with the aid of graphical displays that further highlight the practical utility of this approach.

Several paths for future research remain open. One interesting direction would be to extend this methodology to high-dimensional settings. Combining the cellwise robustness of our approach with regularized covariance estimation might provide a powerful tool for large applications. Additionally, investigating different distributional assumptions could further broaden the scope of the methodology.

Software availability. A zip file with the R code, an example script, and datasets is at https://wis.kuleuven.be/statdatascience/code/cellda_r_code.zip.

References

- Aerts, S. and I. Wilms (2017). Cellwise robust regularized discriminant analysis. *Statistical Analysis and Data Mining* 10(6), 436–447.
- Alqallaf, F., S. Van Aelst, V. J. Yohai, and R. H. Zamar (2009). Propagation of outliers in multivariate data. *The Annals of Statistics* 37(1), 311–331.
- Becquart, C., A. Archimbaud, A. Ruiz-Gazen, L. Pril c, and K. Nordhausen (2026). Invariant coordinate selection and Fisher discriminant subspace beyond the case of two groups. *Journal of Multivariate Analysis* 211, 105521.
- Croux, C. and C. Dehon (2001). Robust linear discriminant analysis using S-estimators. *The Canadian Journal of Statistics* 29, 473–492.
- Croux, C. and V.  llerer (2016). Robust and sparse estimation of the inverse covariance matrix using rank correlation measures. In *Recent Advances in Robust Statistics: Theory and Applications*, edited by C. Agostinelli, A. Basu, P. Filzmoser, and D. Mukherjee, pp. 35–55. Springer.
- Filzmoser, P., K. Hron, and M. Templ (2012). Discriminant analysis for compositional data and robust parameter estimation. *Computational Statistics* 27, 585–604.
- He, X. and W. Fung (2000). High breakdown estimation for multiple populations with applications to discriminant analysis. *Journal of Multivariate Analysis* 72, 151–162.
- Hubert, M. and K. Van Driessen (2004). Fast and robust discriminant analysis. *Computational Statistics & Data Analysis* 45(2), 301–320.

- Nakai, K. (1991). Yeast. UCI Machine Learning Repository. DOI: <https://doi.org/10.24432/C5KG68>.
- Pinheiro, D., M. R. Oliveira, I. Kravchenko, and L. Oliveira (2025). Interval Fisher’s discriminant analysis and visualisation. *ArXiv preprint* 2512.11945.
- Raymaekers, J. and P. J. Rousseeuw (2024). The Cellwise Minimum Covariance Determinant Estimator. *Journal of the American Statistical Association* 119(548), 2610–2621.
- Raymaekers, J. and P. J. Rousseeuw (2025). `cellWise`: Analyzing data with cellwise outliers, CRAN, <https://CRAN.R-project.org/package=cellWise>.
- Raymaekers, J., P. J. Rousseeuw, and M. Hubert (2022). Class maps for visualizing classification results. *Technometrics* 64(2), 151–165.
- Rousseeuw, P. J. and W. Van den Bossche (2018). Detecting Deviating Data Cells. *Technometrics* 60(2), 135–145.
- Rousseeuw, P. J. and K. Van Driessen (1999). A Fast Algorithm for the Minimum Covariance Determinant Estimator. *Technometrics* 41, 212–223.
- Templ, M., K. Hron, and P. Filzmoser (2020). `robCompositions`: an R-package for robust statistical analysis of compositional data, CRAN, <https://CRAN.R-project.org/package=robCompositions>.
- Zaccaria, G., L. Benzakour, L. A. García-Escudero, F. Greselin, and A. Mayo-Íscar (2026). Robust fuzzy clustering with cellwise outliers. *International Journal of Approximate Reasoning* 195, 109698.
- Zaccaria, G., L. A. García-Escudero, F. Greselin, and A. Mayo-Íscar (2025). Cellwise Outlier Detection in Heterogeneous Populations. *Technometrics* 67(4), 643–654.

Supplementary Material to:
Cellwise Robust Discriminant Analysis

A Additional simulation results

A.1 Quadratic discriminant analysis

Here we show the results of the counterpart of the simulation study in the main text, this time in $d = 5$ dimensions. Everything else is set up in the same way.

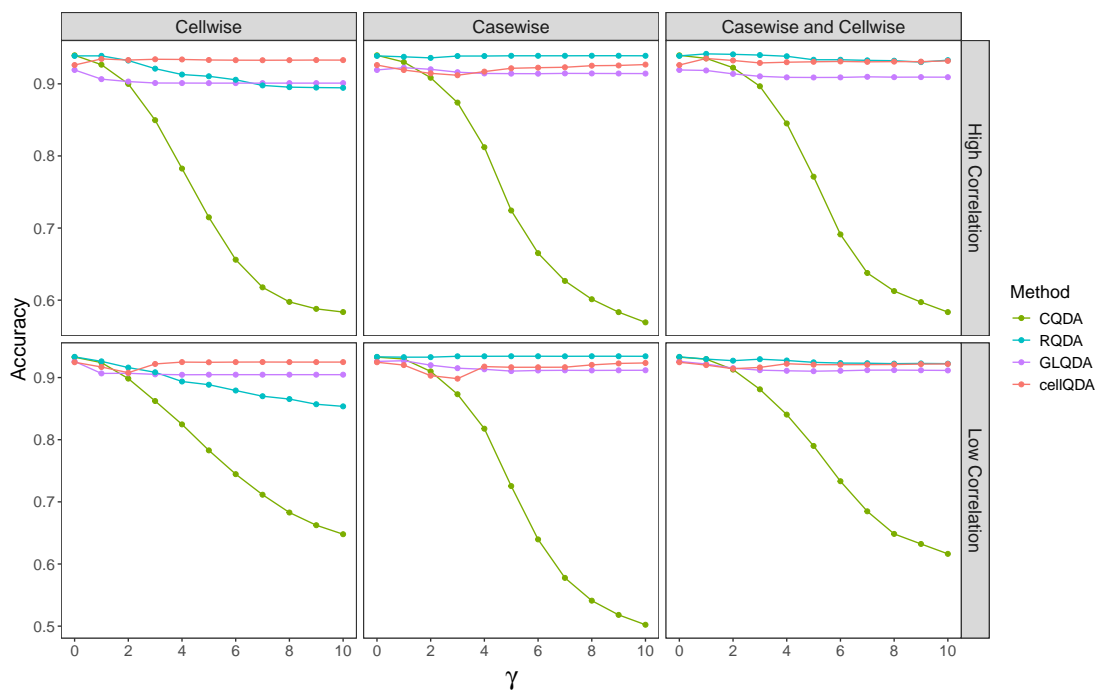


Figure 13: Accuracy of four QDA methods on 3 classes in 5 dimensions, with $n = 200$. In the top row the classes have high within correlations, and the bottom row has low within correlations. The first column uses training data with 10% of cellwise outliers only, the second with 10% of casewise outliers only, and the third with 5% of cellwise and 5% of casewise outliers. The parameter γ on the horizontal axis says how far away the outliers are. The accuracy is measured on test data that contains no contamination.

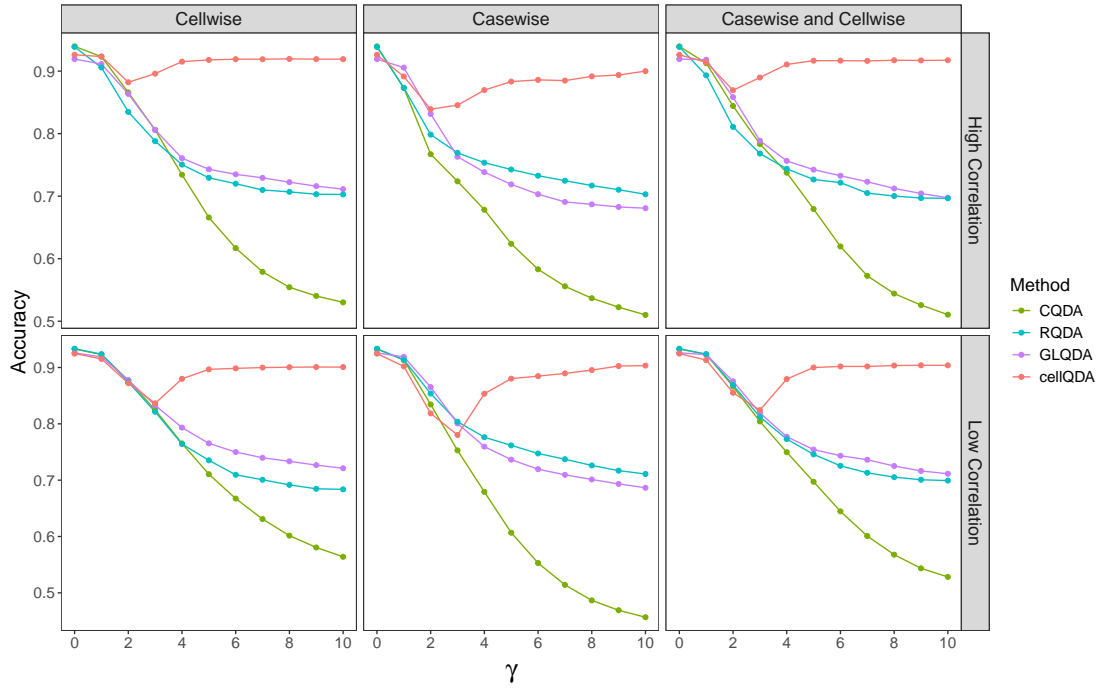


Figure 14: Same training data and fit as in Figure 13, but now the test data has 10% of outlying cells only.

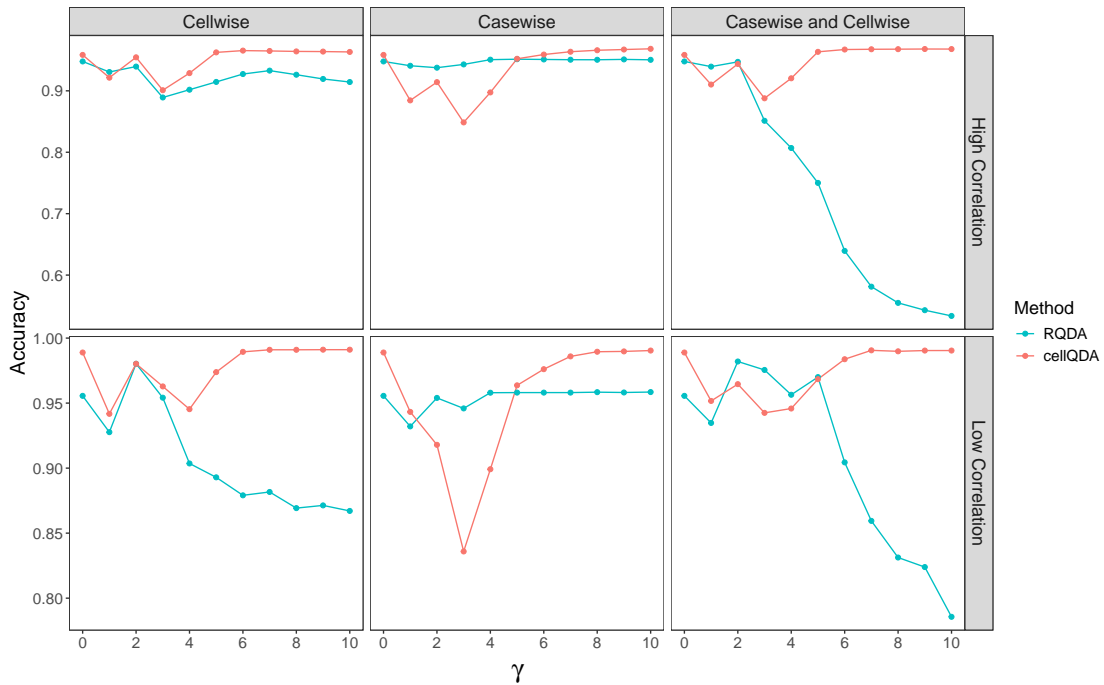


Figure 15: Comparison of RQDA and cellQDA on the same training data as in Figure 13 and displayed in the same way. Now the test data contains a class 0 with 10% of generated casewise outliers. The reported accuracy is of the assignments to the four classes 0, 1, 2, and 3.

A.2 Linear discriminant analysis

In the main text, Figure 7 showed the accuracy of the LDA methods when the test data has 10% of cellwise outliers only. We will now look at the other kinds of test data, also for $d = 20$.

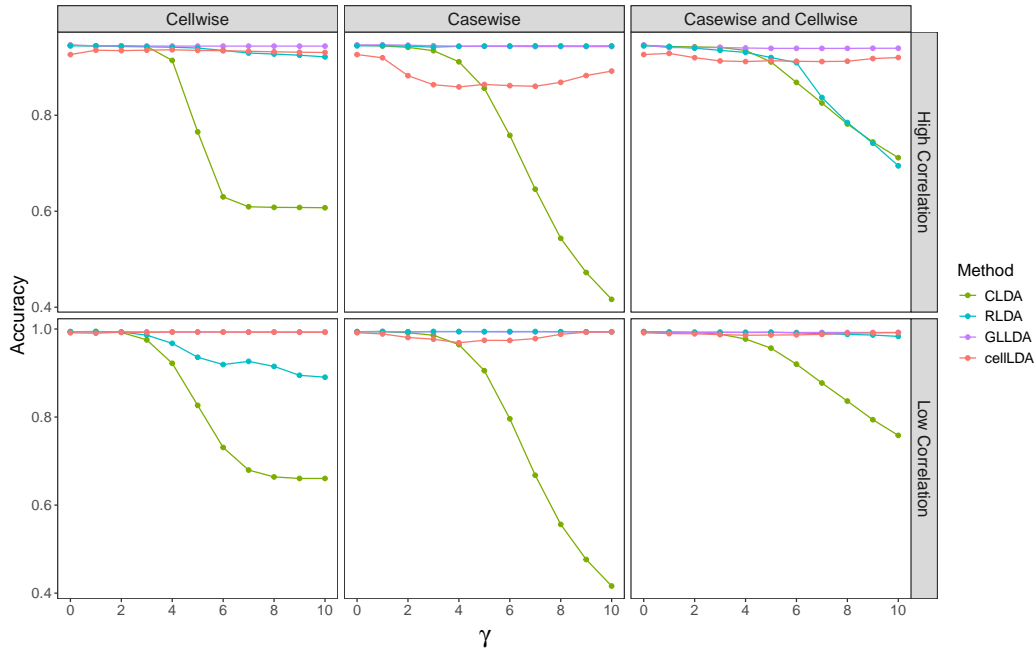


Figure 16: Like Figure 7 with the same training data, but here the test data are clean.

We conclude that in $d = 20$ dimensions, the effects of outliers on the LDA methods are similar to those on the corresponding QDA methods.

Below we see that the situation is similar for $d = 5$ dimensions.

Overall, the effects of cellwise and casewise outliers in 5 dimensions are similar to those in 20 dimensions, and those on LDA are similar to those on QDA.

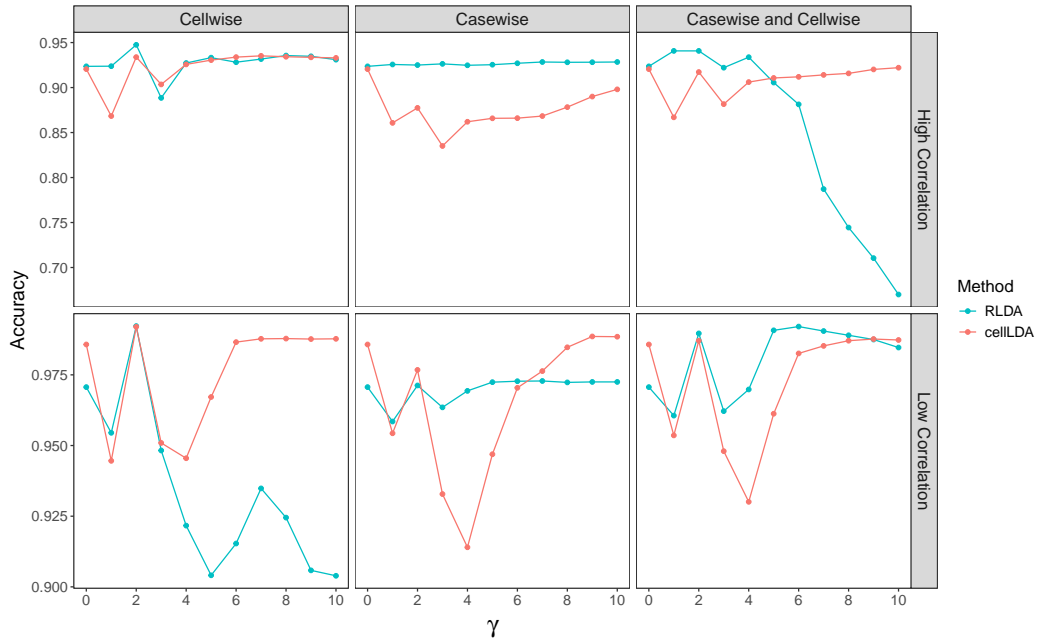


Figure 17: Like Figure 7 with the same training data and estimates, but now the test data has 10% of outlying cases only.

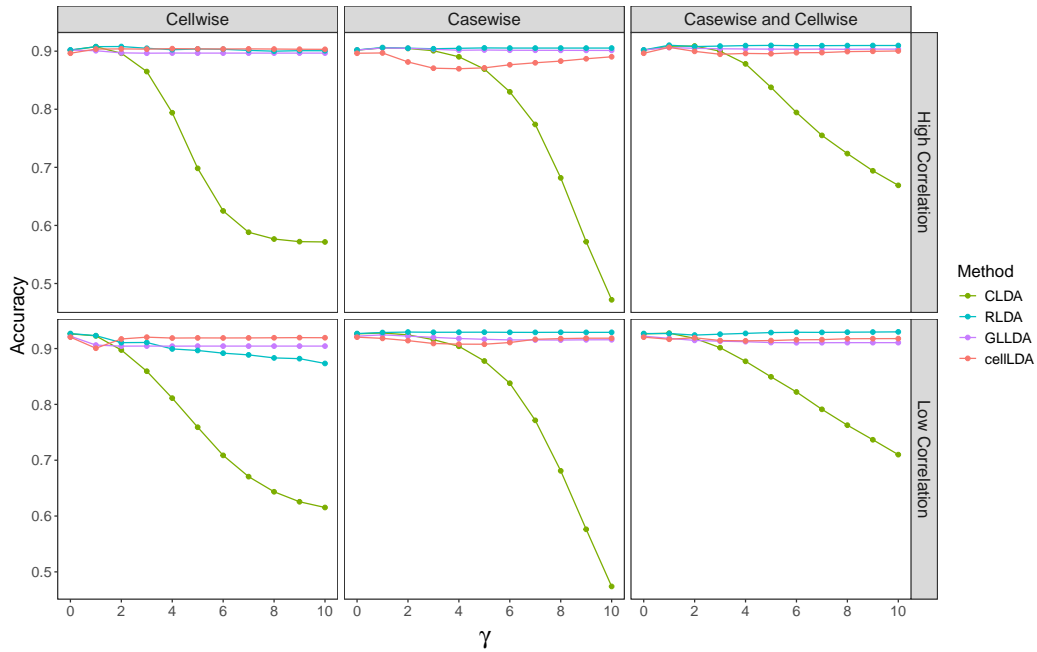


Figure 18: LDA. Like Figure 16 with clean test data, but for $d = 5$.

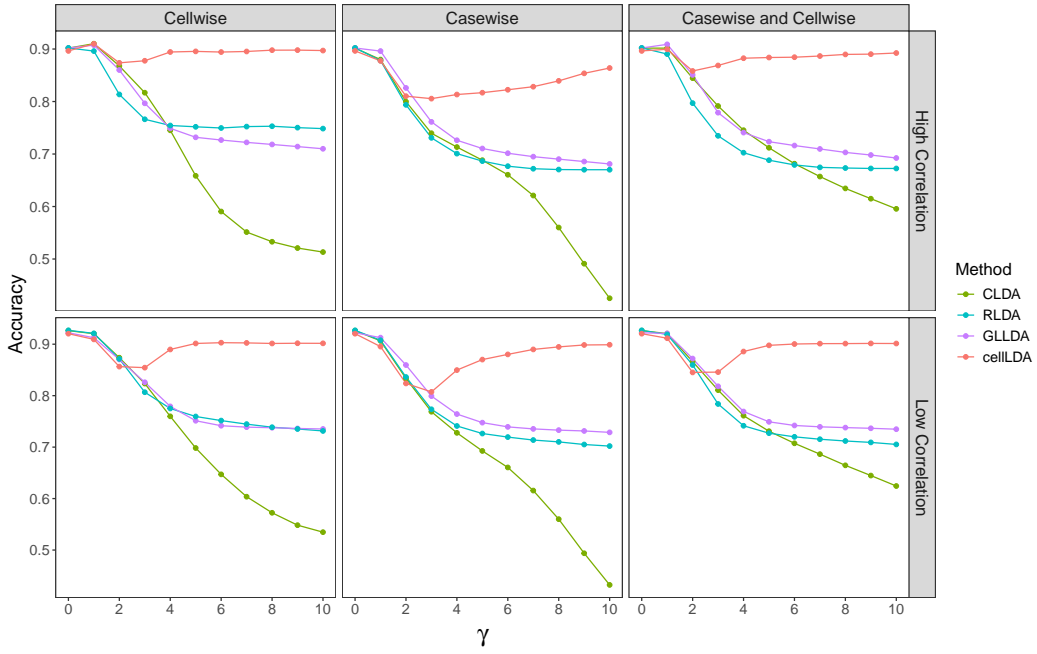


Figure 19: LDA. Like Figure 7 with test data containing cellwise outliers, but for $d = 5$.

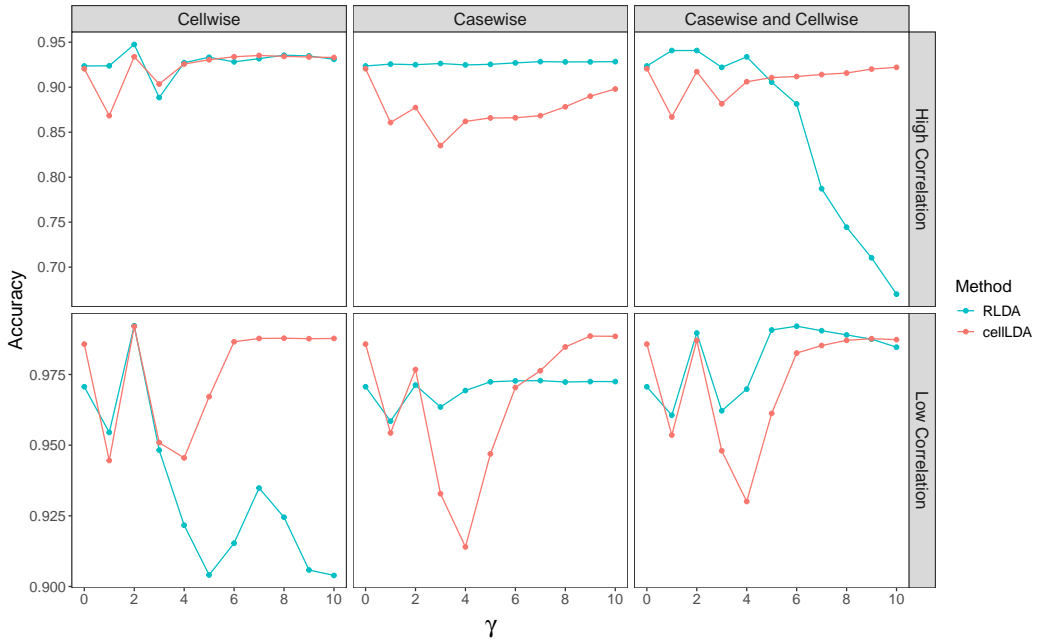


Figure 20: LDA. Like Figure 17 with test data containing casewise outliers, but for $d = 5$.

B Additional Results on the sweets data

In the main text we analyzed the sweets data with cellQDA only. Here we also look at the results of the methods that we compared with in the simulation study. We randomly split off a test dataset with 162 cases (that is, one fifth of the data), and trained on the remainder. Table 1 shows the confusion matrices on the test data.

Table 1: Confusion matrices on test data. The rows contain the given classes, and the columns contain the predictions. Here the class 0 assignment of cellQDA and RQDA is turned off.

Method	<i>True class</i>	<i>Predicted class</i>			
		biscuits	ice cream	cakes	puddings
CQDA	biscuits	30	4	19	0
	ice cream	0	42	2	0
	cakes	0	9	33	0
	puddings	2	20	0	1
RQDA	biscuits	47	0	6	0
	ice cream	0	36	6	2
	cakes	2	0	40	0
	puddings	2	2	5	14
GLQDA	biscuits	48	0	5	0
	ice cream	0	42	2	0
	cakes	4	7	31	0
	puddings	2	19	2	0
cellQDA	biscuits	47	0	6	0
	ice cream	0	35	4	5
	cakes	2	0	40	0
	puddings	2	2	4	15

Note that CQDA almost never assigns a product to the puddings class, instead most puddings are classified as ice cream. It also classifies many biscuits as cakes. GLQDA did

not assign any product to the puddings class. In contrast, the confusion matrices of RQDA and cellQDA are dominated by their diagonals, meaning that most products were assigned to the correct class.

The same effects are visible in more detail in the classmaps of these methods, shown in Figures 21-23.

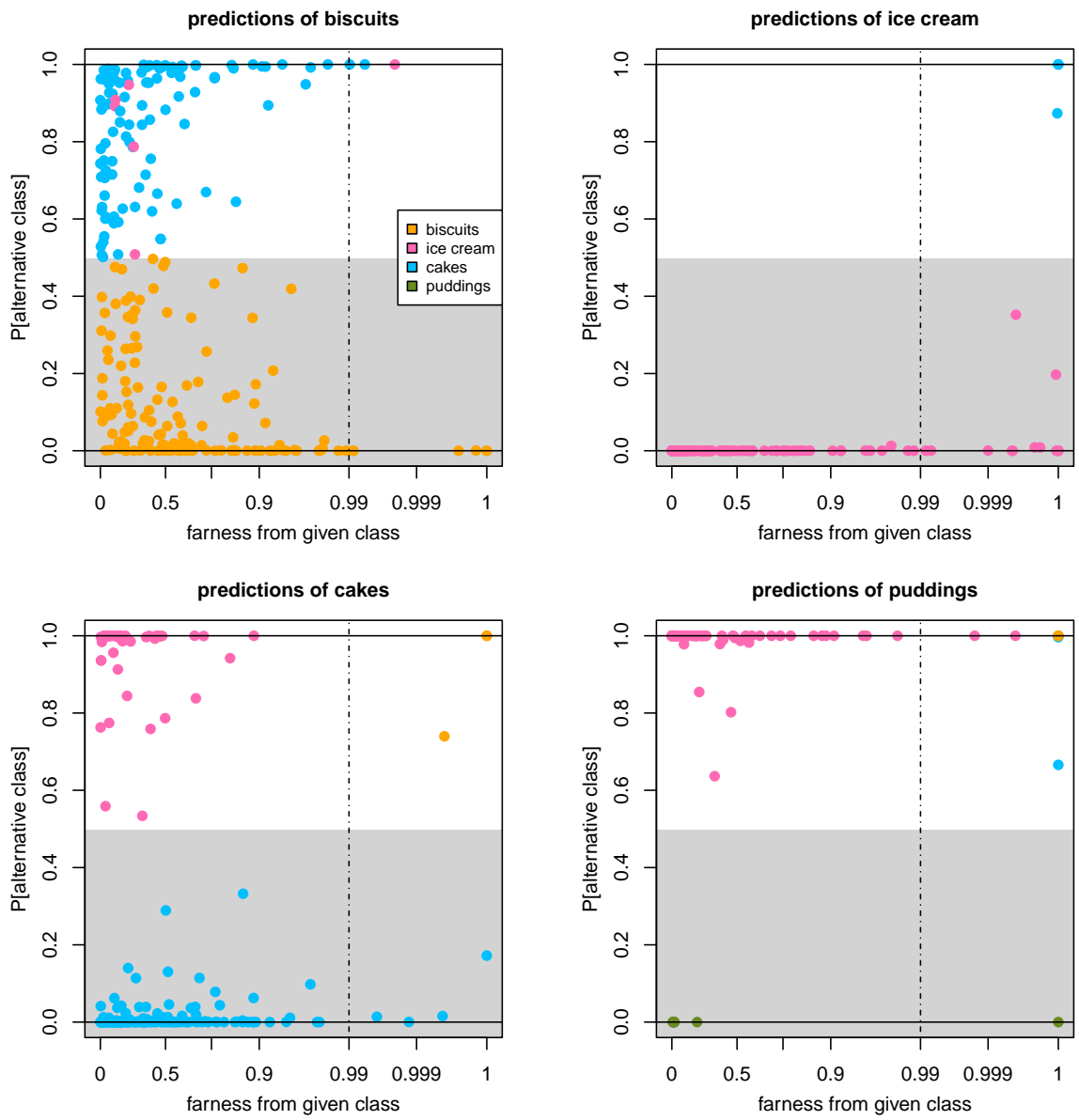


Figure 21: Classmap of CQDA on the sweets data.

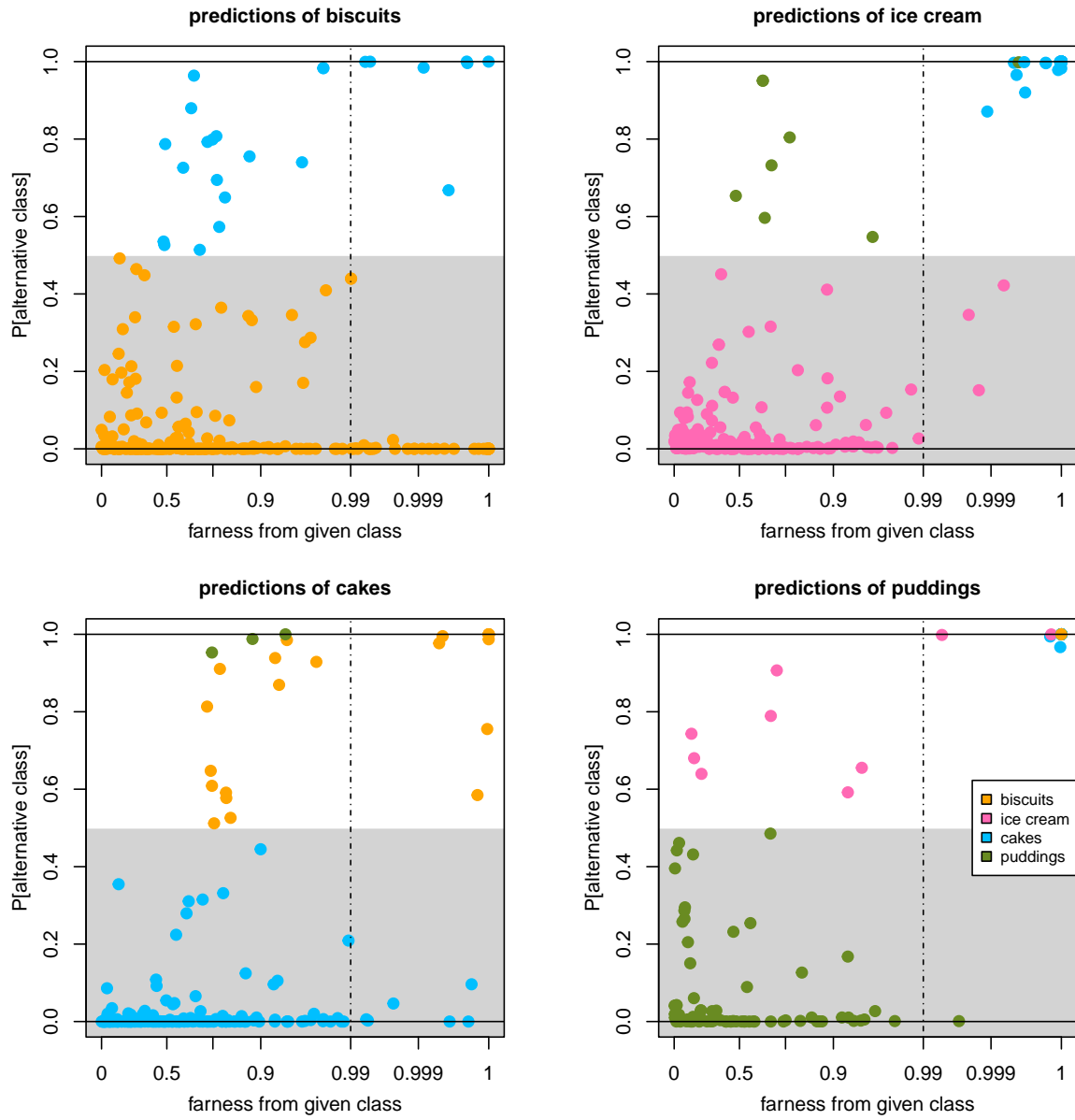


Figure 22: Classmap of RQDA on the sweets data.

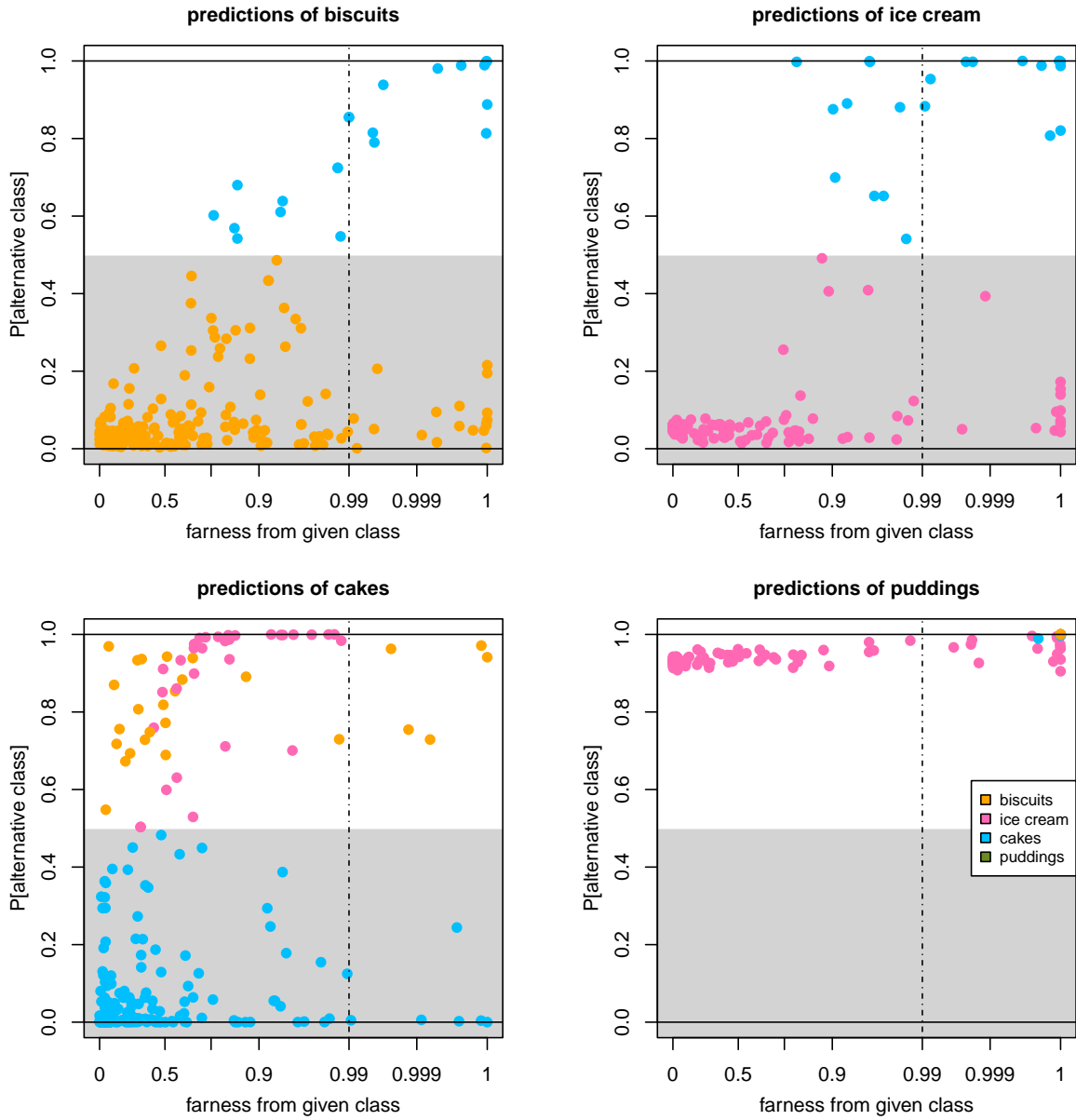


Figure 23: Classmap of GLQDA on the sweets data.

C Two other examples

C.1 Phoneme dataset

The phoneme dataset contains digitized speech signals used to distinguish between nasal and oral phonemes. It has been analyzed in the literature on regularized discriminant analysis, including the work of Aerts and Wilms (2017). Our analysis uses $d = 20$ features that correspond to 20 different log-periodogram frequencies, and $n = 1000$ cases. The original

dataset is publicly available on <http://www-stat.stanford.edu/ElemStatLearn>. The subset used here can be downloaded from https://wis.kuleuven.be/statdatascience/code/cellda_r_code.zip.

We conduct two experiments. First, we compare all four methods on the original data to assess their baseline classification performance. There the 5-fold cross-validation accuracy of cellQDA is 0.815, and exceeds those of CQDA (0.762), RQDA (0.764), and GLQDA (0.772) that lie close together.

Second, we artificially contaminate the data with both cellwise and casewise outliers as in the simulation design in Section 3, but now based on the estimated $\hat{\mu}_g$ and $\hat{\Sigma}_g$ as we have no true values. We generate 5% of cellwise outliers and 5% of casewise outliers. The accuracy was obtained from 5-fold cross-validation, that was repeated 10 times. The casewise outliers were excluded from the test folds, in order to enable a fair comparison across methods with different outlier detection capabilities.

In Figure 24 we see that contaminating the data does not affect cellQDA much, but the other methods suffer from it, especially as γ increases.

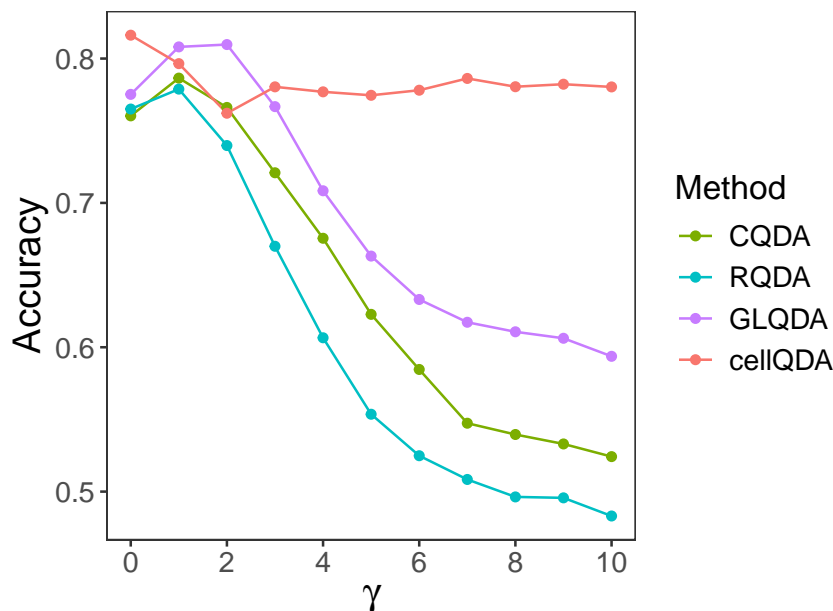


Figure 24: Cross-validated accuracy on the phoneme data. For $\gamma = 0$ we used the original data. For $\gamma > 0$, we inserted 5% of cellwise and 5% of casewise outliers.

C.2 Yeast dataset

The yeast dataset is a widely used benchmark for protein localization prediction (Nakai, 1991). The original data contain 10 classes, corresponding to different cellular localizations, but several classes have very few cases. We restrict our analysis to the three largest classes: CYT (cytosolic), NUC (nuclear), and MIT (mitochondrial), yielding a total of $n = 665$ cases. We also remove three variables from the analysis. The variables `er1` and `pox` are excluded because they are nearly constant across all cases. The variable `nuc` exhibits irregular behavior: it is discrete or even constant in some classes rather than continuous, so it is excluded too. After these preprocessing steps, $d = 5$ variables remain. The original dataset is publicly available through the UCI Machine Learning Repository at <https://doi.org/10.24432/C5KG68>. The subset can be downloaded from https://wis.kuleuven.be/statdatascience/code/cellda_r_code.zip.

We carry out the same experiments as on the phoneme dataset. On the original data, the accuracy of cellQDA is 0.627, and exceeds those of CQDA (0.532), RQDA (0.614), and GLQDA (0.478). All accuracies are fairly low on these data, because the classes CYT and NUC overlap substantially. Figure 25 indicates that the accuracy of cellQDA is not affected much by the added contamination.

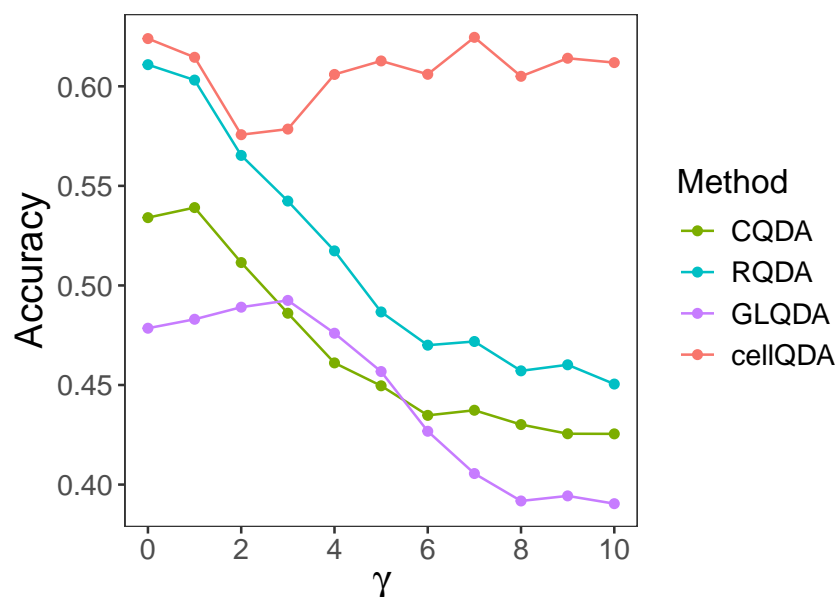


Figure 25: Cross-validated accuracy on the yeast data. For $\gamma = 0$ we used the original data. For $\gamma > 0$, we inserted 5% of cellwise and 5% of casewise outliers.